VI. UNDERWATER VEHICLE DYNAMICS MODEL

A. INTRODUCTION

Underwater vehicle design and construction is almost completely preoccupied with environmental considerations. The ocean completely surrounds the vehicle, affects the slightest nuance of vehicle motion and poses a constant hazard to vehicle survivability. Many of the effects of the surrounding environment on a robot vehicle are unique to the underwater domain. Vehicles move through the ocean by attempting to control complex forces and reactions in a predictable and reliable manner. Thus understanding these forces is a key requirement in the development and control of both simple and sophisticated vehicle behaviors. Unfortunately, the underwater vehicle development community has been hampered by a lack of appropriate hydrodynamics models. Currently no single general vehicle hydrodynamics model is available which is computationally suitable for predicting underwater robot dynamics behavior in a real-time virtual world.

The intended contributions of the hydrodynamic model in this dissertation are clarity, analytical correctness, generality, nomenclature standardization and suitability for real-time simulation in a virtual world. Many interacting factors are involved in underwater vehicle dynamics behavior. These factors can result in oscillatory or unstable operation if control algorithms for heading, depth and speed control do not take into account the many complex possibilities of vehicle response. Laboratory modeling of hydrodynamics response to underwater vehicle motion is essential due to the need to avoid control law errors, sensing errors, navigational errors, prematurely depleted propulsion endurance, loss of depth control, or even catastrophic failure due to implosion at crush depth. An analytically valid hydrodynamics model must be based on physical laws and sufficiently accurate for the study and development of robust control laws that work under a wide range of potential vehicle motions. The

real-time hydrodynamics model is therefore an essential component of a robot-centered underwater virtual world.

Detailed analysis of underwater vehicle hydrodynamics behavior is beyond the current state of the art using real-time simulation techniques. In many cases, detailed data on underwater vehicle hydrodynamics response is unavailable even in real world test programs. Development of a general physics-based real-time model fills a gap in the robotics and simulation literature that does not exist for corresponding robot operating environments such as indoors, space or air. Inclusion of an analytically correct and verifiable hydrodynamics model in an underwater virtual world will permit meaningful and timely analysis of realistic robot-environment interactions.

It must be noted that "correctness" may not be rigorously possible for any hydrodynamics model. So many interrelated factors are present that precise testing and verification of all parameters is unlikely or impossible. While a model of hydrodynamics forces may never be perfect, it can achieve sufficiency in that vehicle responses can be predicted by physical laws at a level of detail adequate to develop, test and evaluate vehicle performance under a variety of control laws. The quantifiable goal for correctness in this work is a generalizable model that predicts vehicle physical response with sufficient rapidity and accuracy to permit equivalent robot behavior whether in the laboratory or underwater. Such a model will also enable realistic and repeatable design and evaluation of vehicle control systems, again either in the laboratory or underwater.

The model presented herein was intentionally developed with complete independence from classified U.S. Navy research on vehicle hydrodynamics. No classified documents were consulted during the literature search for this work. Research statements and conclusions are derived solely from the extensive open literature on hydrodynamics, in no way confirming, denying or implying the existence of similar work in the classified arena. A good unclassified tutorial on the fundamentals of naval submarine design is (Jackson 92). Details on experimentally and analytically developing submarine hydrodynamics models are in (Huang 88).

Unclassified overview descriptions of the use of a hydrodynamics model in the design and testing of the ARPA/Navy Unmanned Underwater Vehicle (UUV) are in (Pappas 91) and (Brancart 94). Primary references for this dissertation are (Healey 92c, 93) and (Fossen 94). Finally, a large number of papers and theses have been written at the Naval Postgraduate School (NPS) pertaining to hydrodynamics modeling of the NPS AUV, and each contributed to the theoretical and experimental knowledge presented here (Papoulias 89) (Cristi 89) (Jurewicz 90) (Zyda 90) (Warner 91) (Bahrke 92) (Brutzman 92a) (Brutzman 92c) (Cooke 92a, 92b) (Cody 92) (Brown 93) (Belton 93) (Haynes 93) (Zehner 93) (Cottle 93) (Torsiello 94) and (Marco 95).

This chapter begins with a comparison of dynamics considerations for different vehicles and their respective environments. A description of world and body coordinate systems is used to derive Euler angle kinematics equations of motion. A rigorous real-time six degree-of-freedom hydrodynamics model is then derived based on the work of (Healey 92c, 93) (Fossen 94) and others. Verified coefficient values for the NPS AUV II *Phoenix* vehicle are included and experimental model coefficient determination for other vehicles is considered. Different representations for calculating vehicle motion are compared using Euler angle or quaternion methods. Network protocol considerations are then examined for integration of the hydrodynamics model into a wide-scale distributed virtual world using the Distributed Interactive Simulation (DIS) protocol. A general object-oriented networked underwater rigid body class hierarchy is presented. Simulation of on-board sensors is considered, and the relationship of robust control system design to hydrodynamics modeling is briefly examined. Finally, future work is discussed concerning tether dynamics, ocean current modeling and collision detection. and addition of hydrodynamics models to on-board robot autopilots.

B. COMPARISON OF DYNAMICS FOR GROUND VEHICLES, AIR VEHICLES, SPACE VEHICLES, SURFACE SHIPS AND UNDERWATER VEHICLES

Dynamics models are available for a wide variety of vehicles and articulated bodies (Fu 87) (Greenwood 88) (Wilhelms 91) (Green 91) (Barzel 92) (Witkin 93). In every case it is desirable that the physical laws governing vehicle interaction with its environment be specified as exactly and correctly as possible. Constraints on vehicle motions vary greatly during interaction with different environments. A brief examination of each basic type of vehicle environment and the physics associated with those environments is useful in understanding the nature of hydrodynamics modeling.

One well-specified objective of the hydrodynamics model is to repeatedly determine system state, defined as follows:

> The *state* of a system is a mathematical structure containing a set of n variables $x_1(t),x_2(t),...,x_i(t),...,x_n(t)$, called the *state variables*, such that the initial values $x_i(t_0)$ of this set and the system inputs $u_j(t)$ are sufficient to uniquely describe the system's future response for $t \geq t_0$. There is a minimum set of state variables which is required to represent the system accurately. The m inputs, $u_1(t),u_2(t),...,u_i(t),...,u_n(t)$, are deterministic; i.e., they have specific values for all values of time $t \geq t_0$. (D'Azzo 88)

An alternative definition of state is the minimum set of variables from which the position, orientation and combined kinetic and potential energy of the vehicle can be determined uniquely. Unique descriptions of vehicle state also require inclusion of an accompanying dynamics model, consisting of an equal number of simultaneous equations as there are state variables expressed in list order form. One further clarification of the quoted definition is that input forcing functions need not be deterministic and can be stochastic.

A key characterization of any set of dynamics laws is whether the system is holonomic or nonholonomic. These two terms are frequently misunderstood and merit definition here. *Holonomic* describes motion that includes no constraints between any

of the independent state variables of a rigid body; literally, the motion is "whole." Ordinarily, for a single rigid body, twelve state variables pertain to holonomic motion, corresponding to six physical degrees of freedom. Specifically these twelve state variables include six values for linear and rotational velocities, and six values for position and orientation (i.e. posture). *Nonholonomic* motion indicates that there are interdependent constraints on rigid body motion, or that variation in one or more of these state variables is dependent upon or constrained by other state variables. Nonholonomic constraints prevent direct integration of accelerations and velocities into posture. Examples of nonholonomic motion constraints include a rolling ball that can not slip (i.e. lose traction) relative to a surface, or parallel parking an automobile where no sideslip is allowed. Another example is a falling cat as it moves in midair, which must obey the conservation law for angular momentum. In each case, nonholonomic constraints limit the freedom of motion. Further descriptions and recent research in nonholonomic motion are examined in (Greenwood 88), (Latombe 91) and (Li, Canny 93).

1. Ground Vehicles

Ground vehicles are constrained by contact with a surface that generates normal and frictional forces between vehicle and terrain. On a surface that is predominantly planar, high frequency vertical components of motion are relatively small contributors to horizontal motion, particularly since they may be intentionally damped or compensated for by mechanical devices such as shock absorbers, tire wheels, suspension systems or flexible legs. Vertical forces merely displace the vehicle a small and independent amount in the vertical direction with little effect on horizontal velocity. Travel up and down hills can add a vertical component to the direction of motion but does not fundamentally change the two-dimensional nature of vehicle travel relative to the surface. Often simple kinematic models suffice for wheeled robots (Alexander 90), especially when surface vehicle motion is slow and constrained to follow roads and tracks when outside or flat floor surfaces when

indoors. Legged robot interactions with surfaces are complex and require dynamics models (Frank 69) (McGhee 79) (Raibert 86).

Ground vehicle motion is complicated by operation at the interface between two media: ground and atmosphere. Aerodynamics loading is usually secondary, but must be considered during high wind conditions or in conjunction with the response at high relative speeds between robot and ground. Detailed analysis of the mechanisms governing vehicle interaction with various surface types is extremely complex, particularly during traversal of rough terrain by off-road vehicles (Bekker 56) (Bekker 69). Fortunately for most robot operations, however, the dynamics of ground-vehicle interaction rarely has a direct bearing on vehicle stability, reliability, navigation or higher-level control functions. Ground robots may further attempt to take advantage of ground contact for navigational purposes by measuring wheel rotation, frictional contact or leg motion (MacPherson 93). In this overall robotics context, regardless of how motion is estimated, ground vehicle dynamic behavior is often well approximated by kinematic models, with dynamics considerations typically having only secondary effects on robot control logic. Ground vehicles remain highly constrained by the nonholonomic nature of contact between vehicle and environment.

2. Air Vehicles

Air vehicles differ from ground vehicles in that vertical components of motion are coupled to interactions in the local horizontal plane. Interactions with the atmosphere due to aerodynamic forces have a significant effect on vehicle motion. There is no direct constraint on air vehicle posture analogous to ground contact, and aircraft flight dynamics are holonomic. Fixed wing air vehicle dynamics are typically dominated by the high speed forward motion which is necessary to generate sufficient lift to carry vehicle weight. The density of air is low, and thus vehicle accelerations do not produce significant acceleration-related aerodynamic forces. This means that the atmosphere does not induce significant "added mass" effects (Yuh 90).

Helicopters differ in many respects from fixed wing aircraft. Helicopter rotors have high degrees of freedom due to multiple rotor blades, each of which have

individual mechanical articulations for twist and lag. Additional degrees of freedom occur due to many factors, including flexible rotational twist of individual blades, tail rotors, optional jet assist, and airstream interactions during phenomena such as turbulence and ground effects. Despite this high degree of complexity, helicopter dynamics can be well specified (Saunders 75), modeled in real time (Williams 85) (Offenbeck 85) and visually verified during repeated testing.

In fixed-wing aircraft, wings support the weight of the vehicle and also support control surfaces. Although aircraft weight and balance variations can produce large effects, they are ordinarily maintained within carefully specified ranges that the wings and control surfaces can accommodate. Wing aerodynamics have been extensively studied under steady motion conditions and are easily generalizable. Thus the overall lift and drag behavior of most air vehicles can be predicted with reasonable accuracy and in real time using simultaneous differential equation solutions (Cooke 92a, 92b) (Rolfe 86). Nevertheless precise localized modeling of high-performance aircraft dynamics for design purposes does not permit general closed-form solutions. Feasible solutions for precision design include massive finite element analysis, a large-scale computational fluid dynamics (CFD) approach, and wind tunnel testing. These approaches do not suit real-time application since large-scale finite element analysis and CFD are considered computational "grand challenges" (Draper 94). Scientific visualization and virtual reality techniques have also been applied with some success in advanced aircraft design (Bryson 91). These complex advanced techniques are special cases, however, compared to the general state of the art in aircraft design. Aircraft dynamics are typically well defined, well understood, and directly verifiable through visual examination during in-flight tests and wind tunnel experiments.

3. Space Vehicles

Space vehicle dynamics are principally determined by orbital mechanics. Friction between vehicle and environment is almost non-existent, and thus the equations of motion include only gravitational, inertial and thrust effects. There are

few (if any) uncertain vehicle parameters, and vehicle postures can be tracked both locally and remotely with great precision. Interestingly, ballistic missiles can be considered a special class of orbital vehicle whose path intersects the Earth's surface (Bate 71). Many summaries of spacecraft dynamics are available, including (Larson 92) (Bate 71) (Allen 91). Translation and angular movements for orbital vehicles may be counterintuitive from an everyday perspective but can be calculated exactly. Under some conditions this motion can be nonholonomic, since six degree-of-freedom space vehicles controlled by internal motors must still conserve angular momentum. If thrusters are used, spacecraft motion is holonomic. Additionally some orbital vehicles (such as an astronaut in a space suit) have a variable mass distribution and may not strictly behave as rigid bodies. Other motions at higher frequencies may exist if vehicle components are flexible, in which case detailed partial differential equation solutions are required for twist, bending, shear and axial deformation. Nevertheless, in many respects the mathematical and empirical foundations of equations predicting spacecraft motion are the best defined, best understood and most directly verifiable of any vehicle type.

4. Surface Ships

Surface ship dynamics are unconstrained in six degrees of freedom and are holonomic. The vertical component of motion is primarily determined by very large counterbalancing values of weight and displacement which keep the ship at the surface of the ocean. Vertical posture changes due to pitch and roll variations normally average to zero over long time scales, due to the hydrostatic righting moments produced by the current location of the center of buoyancy relative to the center of gravity. Equipment, personnel and overall ship trajectory are typically unaffected by the time rates of change of components of motion, either by design or seafaring practice. Changes in vertical motion are strongly affected by the changing buoyancy of the vehicle which varies as water displacement changes. As a result, a paramount criterion in ship design is that the vehicle be reliably stable and self-righting, under both normal and damaged conditions. Interactions of greatest interest between vehicle

and environment usually pertain to the travel of the ship along the horizontal ocean surface. Nevertheless motion is greatly complicated by vehicle operation at the interface between two media: ocean and atmosphere. Except for sailing vessels and ships with low headway, aerodynamic forces tend to be weaker than hydrodynamic forces. Regardless of surface ship type, both sets of forces can be significant and both must be considered simultaneously.

Hydrodynamics and navigation of surface vessels are complex subjects but have been extensively studied, with a comprehensive compendium of knowledge in (Lewis 88) and more examples in (Fossen 94) (Covington 94) (Maloney 85). Predictable courses, predictable speeds, sideslip (lateral motion due to momentum during turns) and gradual smooth changes in vehicle velocity are all typical of surface ship behavior. Behavior of surface vehicle dynamic response can be tested and verified visually. Tow tank verification is also possible, but tow tank testing is expensive and is limited by two competing requirements. Test tank model designers attempt to maintain inverse proportionality constraints between the square root of model scale and maximum water speed (Froude number), along with the concurrent desirability of simultaneously maintaining drag coefficient (Reynolds number) similarity. Tradeoffs between these competing requirements are necessary when building and testing scale models. Wind and wave models can be represented by complex spectral functions that are computationally expensive and difficult to specify (Fossen 94). Nevertheless environmental disturbances can be separately computed and independently added to hydrodynamic forces based on the principle of superposition (Lewis 88) (Fossen 94). Additionally, linear models are available for wind and wave behavior which permit reasonably accurate real-time simulation (Fossen 94) (Covington 94). Models of similar or lesser complexity are also available for hovercraft vehicles (Amyot 89). In summary, modeling of surface ship dynamics is reasonably well defined, well studied and directly verifiable during testing.

5. Underwater Vehicles

Underwater vehicle dynamics may be as complex and difficult to model as any of these regimes, principally due to difficulties in observing and measuring actual underwater vehicle hydrodynamics response. Submerged vehicle motion is not constrained in the vertical direction. For some unmanned vehicles, posture must be restricted to only reach moderate pitch and roll angles. This constraint is imposed since pointing vertically or inverting can cause equipment damage or dangerous control response. Very large angles of attack between vehicle orientation and vehicle direction of motion are possible. The effects of forces and moments can all be cross-coupled between vertical, lateral and horizontal directions. Motion in world coordinates is only calculable after all effects in the body coordinate system are comprehensively predicted. Actual vehicle motion can be watched remotely only with very low precision or (more often) not at all. Tow tank testing imposes unrealistic external force constraints which are otherwise not present. The effects of the surrounding environment are relatively large and significant, so much so that the adjacent water tends to be accelerated along with the vehicle and can be thought of as an "added mass." Together these challenges make underwater vehicle physical response, guidance and control an extremely difficult dynamics problem.

There are over one hundred pertinent coefficients and variables relating to the linear and non-linear coupled effects of lift, drag, added mass and propulsion in the model of this dissertation. Although a number of these coefficients are of second-order effect or negligible importance, determination of primary coefficient values is very difficult and expensive. These problems are frequently compounded when the subject vehicle has an open frame with irregular surfaces, or when a towed tether is attached.

It is conceivable that an even more complex and fundamental model to calculate underwater vehicle dynamics might be derived than is presented here. Specifically, the Navier-Stokes fluid flow differential equations might be applied in a CFD vehicle-fluid coupled interaction model (Ren 93). Closed-form solutions for this

approach do not exist, and numerical methods attempting to solve the Navier-Stokes partial differential equations in this domain tend to introduce more unknown parameters than they eliminate. This is a particular problem for UUVs which often have irregular shapes. Additionally, CFD problems are among those currently considered as computational "grand challenges" (Draper 94). Thus CFD methods are not currently suitable for real-time simulation of underwater vehicle hydrodynamics.

Many models exist for ground vehicles, air vehicles, space vehicles, and surface ships that appear suitable for real-time use in a virtual world. No complete analogous model for underwater vehicles was encountered during this research. A great many partial models of underwater dynamics exist, but all were found to suffer from incompleteness, confused nomenclature, oversimplification, or a formulation unsuitable for real-time simulation. No other models were found which combined cruise mode hydrodynamics (propellers, fins and predominantly forward velocity) with hovering mode hydrodynamics (thrusters, station-keeping, low forward motion and large angle of attack). *No rigorous general model was previously available from a single source which is computationally suitable for real-time simulation of submerged vehicle hydrodynamics.*

6. Comparison Summary

Examination of the salient characteristics of dynamics models in these many different robot environments reveals that the underwater case is very difficult to accurately specify, most difficult to verify and most critical for preventing catastrophic vehicle loss. Failure to properly predict the dynamics of ground vehicles, orbital space vehicles or surface ships at worst may result in a vehicle which stays in place and can be safely commanded. Failure of aircraft due to improper prediction of aerodynamics can be mitigated through well-developed analytic techniques, wind tunnel testing and remote human supervisory control. Failure to properly predict the dynamics of underwater vehicles can lead to overall system failure due to any number of subsequent related faults in control, sensing, navigation or power consumption. This critical vulnerability in underwater vehicle design is a contributing cause to the relative

rarity of working underwater robots. Thus the rigorous and nearly complete (Healey 93) hydrodynamics model, which is compatibly described in (Fossen 94), has been fully extended and implemented here. This revised hydrodynamics model now fills a significant gap in the robotics and simulation literatures.

C. COORDINATE SYSTEMS AND KINEMATIC EQUATIONS OF MOTION

Proper definitions of coordinate systems are essential to specifying the physical behavior of vehicles in a fluid medium. There are two coordinate systems which must be understood independently and in relation to each other: world coordinates and body coordinates.

World coordinates are defined with respect to the surface of the earth, and so are sometimes referred to as *earth coordinates* or *inertial coordinates*. A variety of standardized world coordinate systems are now in common use. The world coordinate system of this model is defined by three orthogonal axes originating at an arbitrary local point at the ocean surface. North corresponds to *x*-axis, East corresponds to *y*-axis and increasing depth corresponds to *z*-axis as shown in Figure 6.1. These axes follow right-hand rule conventions, and are identical to (or compatible with) standard world coordinate systems defined in robotics, computer graphics, aircraft aerodynamics, naval architecture, navigation and the Distributed Interactive Simulation (DIS) protocol (Fu 87) (Foley, van Dam 90) (Cooke 92a, 92b) (Lewis 88) (Fossen 94) (Maloney 85) (IEEE 93, 94a, 94b). Conversions from a topocentric local earth coordinate frame to geocentric or geodetic coordinate systems are given in (Lin 93). Other coordinate systems are possible but remain undesirable if they do not match these important standardized conventions.

Body coordinates are defined with respect to the body of the vehicle of interest. The three axes of a vehicle are longitudinal pointing in the nominal forward direction of the vehicle, lateral pointing through the right hand side of the level vehicle, and downward through the nominal bottom of the vehicle. The origin of body coordinates for a submerged vehicle is at the half point along the symmetric longitudinal axis.

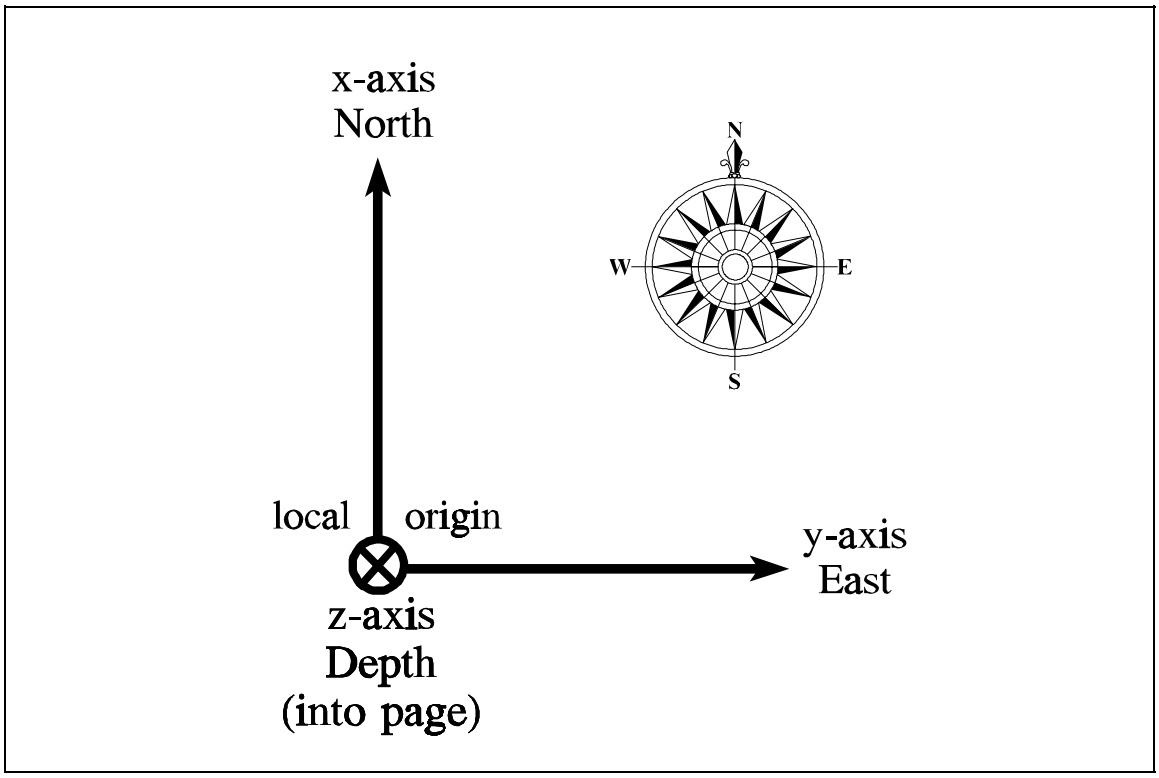

Figure 6.1. World coordinate system.

Typically this point is at or near the *center of buoyancy* (***CB***), which is the centroid of volumetric displacement of the submerged vehicle. A related location is the *center of gravity* (***CG***), which is the first moment centroid of vehicle mass. Ordinarily the center of gravity of a rigid body is the point at which net forces and moments are assumed to be applied. The center of gravity of a ship or submarine is always designed to be below the center of buoyancy to ensure static vehicle stability. The torque due to any vertical difference between the two centers ***CB*** and ***CG*** is called the *righting moment*. A nonzero righting moment results when the centers of buoyancy and gravity are not aligned vertically, tending to bring the submerged vehicle back to a neutral (typically level) pitch and roll posture. Any submerged vehicle that instead has center of gravity above center of buoyancy is inherently unstable and will tend to invert, even under static conditions.

Underwater vehicles often include free-flood spaces which can equalize with ocean pressure through small openings, all while remaining essentially contained by the hull. The water enclosed in these free-flood spaces directly contributes both to volumetric displacement and vehicle mass. Thus free-flood spaces affect buoyancy, mass, center of buoyancy, center of mass and vehicle hydrodynamics response. While submerged these effects are ordinarily static and not time-varying.

Interactions between a vehicle and the ocean environment are defined from the perspective of the vehicle, i.e. within the body coordinate system. This is because all actions and reactions between vehicle and environment are dependent on the orientation, shape, velocity and acceleration of the vehicle body, with the sole exceptions of gravity and ocean current. The direction of gravity can be sensed or estimated and is thus directly usable within the body coordinate frame of reference. Ocean current is reasonably assumed to act uniformly over the entire vehicle body. Therefore all vehicle-environment interactions can first be calculated from the perspective of the floating rigid body located inside a larger homogeneously moving ocean current frame of reference. Wind and surface wave action are normally assumed to have zero effect on submerged vehicles (if they do have an effect, then a surface ship model is likely more appropriate). Conversion from body coordinates to world coordinates consists of angular rotations to align body axes with world axes, correction for vehicle positional translation, and then addition of coordinate displacement due to ocean current motion.

Clear definition of coordinate systems greatly contributes to understanding the kinematics equations of motion. In order to reduce ambiguity, the use of ($\boldsymbol{x}$, $\boldsymbol{y}$, $\boldsymbol{z}$) axis references are in world coordinates except when explicitly stated otherwise. Body axes are referred to as longitudinal, lateral and vertical, corresponding to ($\boldsymbol{x}$, $\boldsymbol{y}$, $\boldsymbol{z}$) body coordinates when an algebraic description is necessary. Strictly defined variables for global coordinate frame translations and orientation rotations appear in coordinate system diagram Figure 6.2. Body coordinate frame linear and angular velocities ($\boldsymbol{u}$, $\boldsymbol{v}$, $\boldsymbol{w}$, $\boldsymbol{p}$, $\boldsymbol{q}$, $\boldsymbol{r}$) are shown in Figure 6.3.

The global coordinate frame *Euler angle* orientation definitions of *roll* (ϕ), *pitch* (θ) and *yaw* (ψ) implicitly require that these rotations be performed in order. Robotics conventions usually specify physical order of rotations, while graphics conventions usually specify temporal order of rotations. Results are identical in each case. When converting from world to body coordinates using physical order (as might be specified in a three-axis gimbal system), the first rotation is for yaw (ψ) about the ***z***-axis, then pitch (θ) about the first intermediate ***y***-axis, then roll (ϕ) about the second intermediate ***x***-axis. Figure 6.4 illustrates these intermediate axes of rotation pertaining to Euler angle rotation (adapted from IEEE 94a). When converting from world to body coordinates using temporal order (as is common in computer graphics), the first rotation is roll (ϕ) about the world reference ***x***-axis, followed by pitch (θ) about the world reference ***y***-axis, and finally yaw (ψ) about the world reference ***z***-axis. Consistency of results using either method can be demonstrated by examining the mathematical order of the resulting rotation matrices, which is identical in each case. Naturally the orders of rotations are reversed if converting from body to world coordinate frame.

These Euler angle definitions are consistent with naval architecture definitions (Lewis 88). This is an important property since twelve different and unique Euler angle coordinate system definitions are possible (Fu 87), while only one Euler angle convention corresponds to naval architecture conventions.

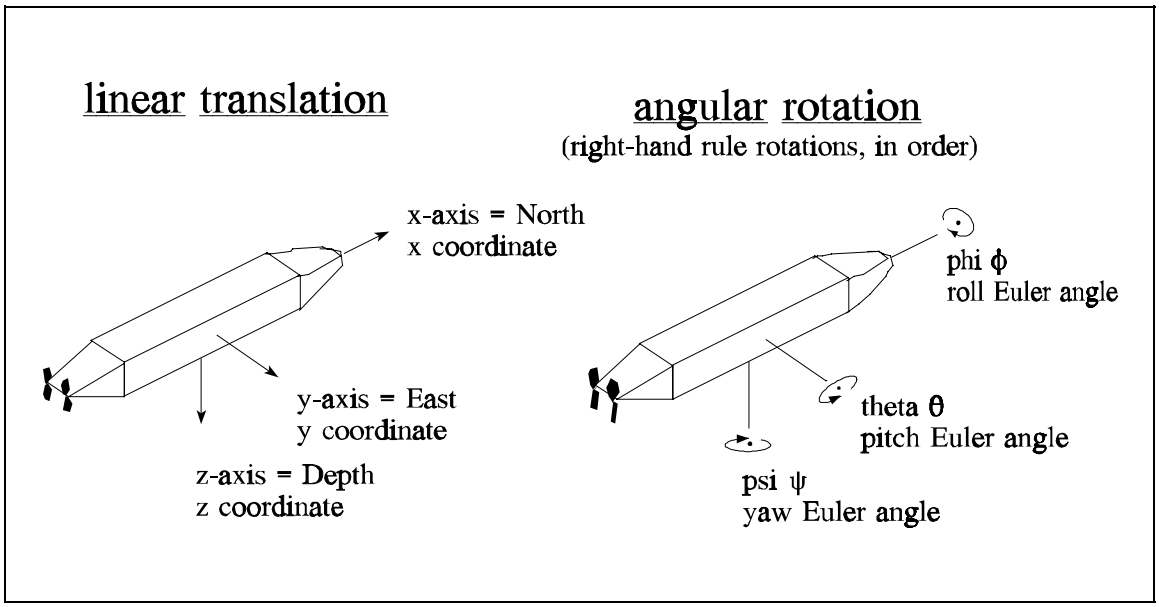

Figure 6.2. World coordinate system: translation and rotation conventions. World x-axis = North, y-axis = East, z-axis = Depth. World-to-body Euler rotations occur in order:
first yaw (ψ), then pitch (θ), then roll (ϕ).

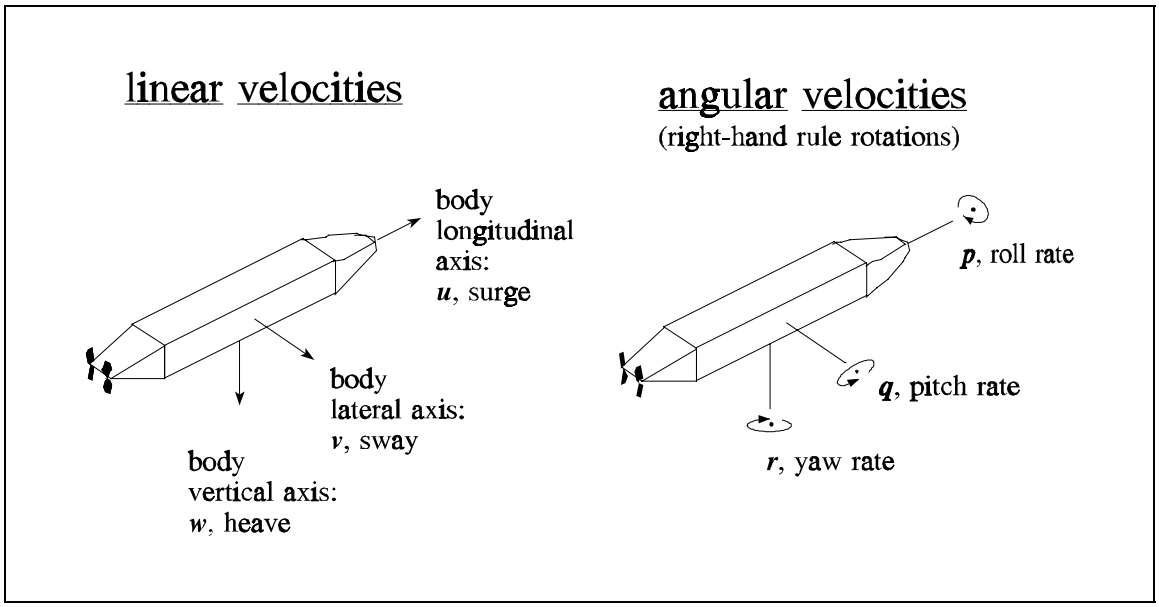

Figure 6.3. Body coordinate system: linear and angular velocity conventions. Note that roll Euler angle rate ≠ roll rate,
pitch Euler angle rate ≠ pitch rate, and
yaw Euler angle rate ≠ yaw rate.

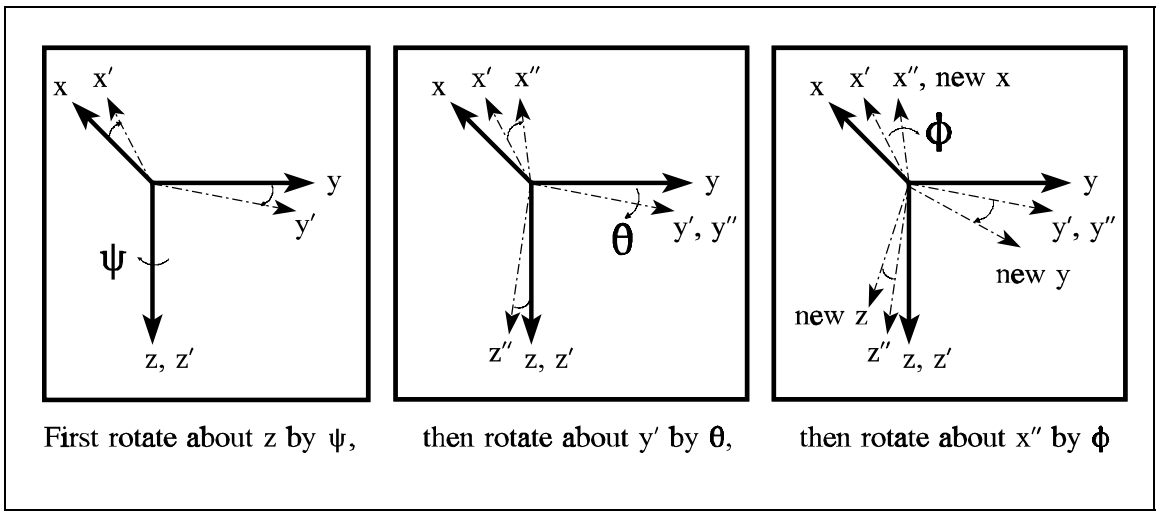

Figure 6.4. Intermediate rotation axes for Euler angle rotations from world coordinate frame to body coordinate frame, adapted from (IEEE 94a).

Normally Euler angles must be restricted from representing a vertical orientation or else mathematical singularities may result. Several techniques for avoiding Euler angle singularities in the vicinity of $\theta = \pm \pi / 2$ are discussed in (Cooke 92a, 92b). Permitted ranges of the Euler angles follow:

$$-\pi < \phi \leq \pi \tag{6.1}$$

$$-\frac{\pi}{2} < \theta < \frac{\pi}{2} \tag{6.2}$$

$$0 \leq \psi < 2\pi \tag{6.3}$$

Additionally, most underwater vehicles must be prevented from inverting horizontally or pointing vertically, in order to prevent internal vehicle damage and uncontrollable maneuvering instabilities. These restrictions add a further constraint on roll angle for

normal operating conditions, but that constraint will not be applied in this model in order to be able to predict vehicle motion under all conditions.

The order of applying roll, pitch and yaw matrix rotations is fixed since these rotations are not commutative. The Euler angle rotation matrices for converting from body to world coordinates follow in Equation (6.4) (Fu 87) (Cooke 92b). Due to typographic errors in a number of other references, matrix multiplication results are also included in Equation (6.5). Finally it is essential to note that, as will be shown, body coordinate frame rotational velocities **p**, **q** and **r** are quite different from the world coordinate frame Euler angle rotation rates $\dot{\phi}$, $\dot{\theta}$ and $\dot{\psi}$.

$$[R] = [R]_{z,\psi}\ [R]_{y,\theta}\ [R]_{x,\phi} \tag{6.4}$$

$$= \begin{bmatrix} \cos(\psi) & -\sin(\psi) & 0 \\ \sin(\psi) & \cos(\psi) & 0 \\ 0 & 0 & 1 \end{bmatrix} \begin{bmatrix} \cos(\theta) & 0 & \sin(\theta) \\ 0 & 1 & 0 \\ -\sin(\theta) & 0 & \cos(\theta) \end{bmatrix} \begin{bmatrix} 1 & 0 & 0 \\ 0 & \cos(\phi) & -\sin(\phi) \\ 0 & \sin(\phi) & \cos(\phi) \end{bmatrix}$$

$$[R] = \begin{bmatrix} \cos\theta\cdot\cos\psi & \sin\phi\cdot\sin\theta\cdot\cos\psi - \cos\phi\cdot\sin\psi & \cos\phi\cdot\sin\theta\cdot\cos\psi + \sin\phi\cdot\sin\psi \\ \cos\theta\cdot\sin\psi & \sin\phi\cdot\sin\theta\cdot\sin\psi + \cos\phi\cdot\cos\psi & \cos\phi\cdot\sin\theta\cdot\sin\psi - \sin\phi\cdot\cos\psi \\ -\sin\theta & \sin\phi\cdot\cos\theta & \cos\phi\cdot\cos\theta \end{bmatrix} \tag{6.5}$$

Since the body to world rotation matrix **[*R*]** is an orthogonal matrix, it follows that **R** inverse equals **[*R*]** transpose.

$$[R]^{-1} = [R]^{T} \tag{6.6}$$

The three world coordinate frame translation rates can be obtained from the body coordinate frame translation rates by the following matrix equation:

$$\begin{bmatrix} \dot{x} \\ \dot{y} \\ \dot{z} \end{bmatrix} = [R] \begin{bmatrix} u \\ v \\ w \end{bmatrix} \tag{6.7}$$

Inversely, body coordinate frame velocities can be determined from world coordinate frame velocities in a similar fashion:

$$\begin{bmatrix} u \\ v \\ w \end{bmatrix} = [R]^T \begin{bmatrix} \dot{x} \\ \dot{y} \\ \dot{z} \end{bmatrix} \tag{6.8}$$

The three world coordinate frame Euler angle rotation rates are obtained from body coordinate frame rotation rates by the following non-orthogonal linear transformations (Cooke 92b):

$$\dot{\phi} = p + q \sin(\phi) \tan(\theta) + r \cos(\phi) \tan(\theta) \tag{6.9}$$

$$\dot{\theta} = q \cos(\phi) - r \sin(\phi) \tag{6.10}$$

$$\dot{\psi} = \frac{q \sin(\phi) + r \cos(\phi)}{\cos(\theta)} \tag{6.11}$$

These three conversions can be combined into matrix notation:

$$\begin{bmatrix} \dot{\phi} \\ \dot{\theta} \\ \dot{\psi} \end{bmatrix} = [T] \begin{bmatrix} p \\ q \\ r \end{bmatrix} \tag{6.12}$$

where

$$[T] = \begin{bmatrix} 1 & \sin(\phi)\tan(\theta) & \cos(\phi)\tan(\theta) \\ 0 & \cos(\phi) & -\sin(\phi) \\ 0 & \sin(\phi)\sec(\theta) & \cos(\phi)\sec(\theta) \end{bmatrix} \tag{6.13}$$

However note that **[*T*]** is not orthogonal, so $[T]^{-1}$ is not calculated by transposition:

$$[T]^{-1} \neq [T]^{T} \tag{6.14}$$

Instead inverse equations for obtaining body angular velocities from Euler angle rates are as follows:

$$p = \dot{\phi} - \dot{\psi}\sin(\theta) \tag{6.15}$$

$$q = \dot{\theta}\cos(\phi) + \dot{\psi}\sin(\phi)\cos(\theta) \tag{6.16}$$

$$r = -\dot{\theta}\sin(\phi) + \dot{\psi}\cos(\phi)\cos(\theta) \tag{6.17}$$

which yield the following matrix equations:

$$\begin{bmatrix} p \\ q \\ r \end{bmatrix} = [T]^{-1} \begin{bmatrix} \dot{\phi} \\ \dot{\theta} \\ \dot{\psi} \end{bmatrix} \tag{6.18}$$

$$[T]^{-1} = \begin{bmatrix} 1 & 0 & -\sin(\theta) \\ 0 & \cos(\phi) & \sin(\phi)\cos(\theta) \\ 0 & -\sin(\phi) & \cos(\phi)\cos(\theta) \end{bmatrix} \tag{6.19}$$

The preceding equations provide a complete set of component conversions between the world coordinate frame and body coordinate frame linear and angular velocities. All component velocities can be further grouped together in matrix notation. Combined velocity matrix definitions are as follows:

$$[V]_{body} = \begin{bmatrix} u \\ v \\ w \\ p \\ q \\ r \end{bmatrix} \tag{6.20}$$

$$[V]_{world} = \begin{bmatrix} \dot{x} \\ \dot{y} \\ \dot{z} \\ \dot{\phi} \\ \dot{\theta} \\ \dot{\psi} \end{bmatrix} \tag{6.21}$$

Matrix conversion from body to world velocities is thus:

$$[V]_{world} = \left[\begin{array}{c|c} [R] & 0 \\ \hline 0 & [T] \end{array}\right] [V]_{body} \qquad \textbf{(6.22)}$$

and inversely:

$$[V]_{body} = \left[\begin{array}{c|c} [R]^T & 0 \\ \hline 0 & [T]^{-1} \end{array}\right] [V]_{world} \qquad \textbf{(6.23)}$$

These velocity relationships are the *kinematics equations of motion* (Greenwood 88). Equations (6.22) and (6.23) are equivalent ways of expressing Euler angle constraints between the inertial world coordinate frame and the rotating body coordinate frame. Each has six component equations linking twelve velocity components. When combined with the dynamics equations of motion, the kinematics equations of motion provide constraints essential to solving world coordinate system values of the vehicle state vector.

D. GENERAL REAL-TIME HYDRODYNAMICS MODEL FOR AN UNDERWATER VEHICLE

1. Definitions

A virtual world simulation component for hydrodynamics modeling of a submerged rigid body must account for six spatial degrees of freedom in real time. The six spatial degrees of freedom include *position* (3 position coordinates ***x***, ***y***, ***z***) and *orientation* (3 rotational Euler angles ϕ, θ, ψ). Together these six components

describe vehicle *posture* (***x***, ***y***, ***z***, ϕ, θ, ψ). Accelerations and velocities each have these same six spatial degrees of freedom.

Six values for velocity and six values for posture comprise the vehicle *state vector*, since together they can fully specify in vehicle posture over time without redundancy. This state vector is in the world coordinate system. The overall goal of the hydrodynamics model is to calculate updated values of the vehicle state vector at each time step.

Much more information is needed to describe robot state. The hydrodynamics model needs a reasonably complete snapshot of robot state in order to properly predict interactions between robot and environment. All hydrodynamics state variables must be included, as well as a variety of sensor values, pertinent robot logic states, and variables for accelerations (due to forces and moments) as produced by effector values for propellers, rudders, planes and thrusters. The dynamics model is provided this partial snapshot of current robot state with each exchange of the robot telemetry record. After examining parameters controlled by the robot (e.g. robot orders for propellers and fins), the hydrodynamics model then calculates an updated state vector. With the updated state vector the hydrodynamics model is then able to calculate values expected from various robot sensors which ordinarily query the environment. By updating missing sensor values in the robot telemetry record with newly calculated sensor values, the hydrodynamics model provides virtual sensor response in the laboratory. Vehicle operation in virtual world or real world remains transparent to the robot. Further details on this data communication mechanism are included in Chapter IV.

2. Real Time

"Real time" in this context is defined by the requirement that a vehicle maneuvering within the virtual world describe essentially the same path and postures as the vehicle maneuvering in the real world. This requires that the robot hardware and software receives the same responsiveness from the virtual world as from the real

world, since robot behavior is very closely coupled to real-time interactions and deadlines (Payton 91) (Badr 92).

> A *real-time system* is a system that must satisfy explicit (bounded) response-time constraints or risk severe consequences, including failure... A *failed system* is a system which cannot satisfy one or more of the requirements laid out in the formal system specification. (Laplante 93)

Real-time systems can be further characterized by the criticality of their timing requirements, which are classified as hard or soft. *Hard real-time* system correctness is strictly dependent on the timeliness of results. *Soft real-time* systems may experience reduced effectiveness but will not fail due to missed deadlines. Alternatively, hard real-time systems are those which include the possibility of system loss or potential catastrophe if deadlines are not met, and soft real-time systems are those where "sooner is better than later" but lateness will not cause system failure. As a point of interest, *firm real-time* systems have been defined as those with hard deadlines that can survive despite the presence of low probabilities for missing a deadline. (Laplante 93) (Halang 91)

By these definitions it is clear that the system consisting of a robot interacting with a dynamics-based virtual world is a hard real-time system. Furthermore the robot itself operating in a real world environment is also a hard real-time system, since a temporal failure in navigation or depth control might result in vehicle destruction. However, in isolation, the dynamics component of the virtual world are able to provide accurate results regardless of the temporal scaling of interaction requests. Therefore the dynamics model *per se* can be classified as a soft real-time system. It only needs to be fast enough to support the hard real-time requirements of the networked robot processors. In general, hydrodynamics model responsiveness will be a function of algorithmic complexity, implementation efficiency, microprocessor performance and communications latency.

3. Forces, Moments and Accelerations

Forces and accelerations for the six state variables of posture can be grouped together in the matrix form of Newton's Second Law, initially expressed as

$$[F]_{world} = \frac{d}{dt}[M\,V]_{world} \tag{6.24}$$

For a rigid body, translational forces are normally applied at the ***CG***. Moments are free vectors producing rotations to be applied about the origin of the vehicle body, since inertial integrals are calculated relative to that origin. Usual practice is to define ***CG*** measurements as being offset from ***CB***. Vehicle origin is not assumed coincident.

The key to properly estimating world coordinate frame velocities and position will be properly calculating time rate of change of velocities in the body coordinate frame, represented as:

$$[\dot{V}]_{body} = \begin{bmatrix} \dot{u} \\ \dot{v} \\ \dot{w} \\ \dot{p} \\ \dot{q} \\ \dot{r} \end{bmatrix} \tag{6.25}$$

Time rate of change of body velocities $[\dot{V}]_{body}$ can also be referred to as *body-relative accelerations* $[A]_{body}$. However it must be clearly understood that these body accelerations are only with respect to the body coordinate frame, i.e. those which appear to a local observer moving with the body reference frame (Greenwood 88). Absolute acceleration components due to rotation and velocity changes between the body reference frame and world reference frame are specifically excluded from $[A]_{body}$.

Since physical interactions occur between the vehicle and the immediately surrounding water volume, force and moment calculations are most directly evaluated in the body-fixed coordinate frame. Moment of inertia terms in the mass matrix **[*M*]** can only be constant in a body coordinate frame, further making the body frame attractive for dynamics calculations. Mathematical rederivation of known acceleration relationships in a world coordinate reference frame is possible using a Lagrangian representation (Fossen 94). However such a form appears to be much less direct than the Newton-Euler formulations, particularly since the virtual world is centered around a robot vehicle which operates and interacts relative to the local body-fixed coordinate frame. Therefore it is desirable that all linear and angular acceleration and velocity relationships be specified exactly and completely in the body coordinate frame. Doing so yields six dynamics equations of motion relating the twelve unknowns of the vehicle state vector derivatives: six unknowns are body velocities, and six unknowns are body accelerations.

Although the vector sum of velocity components expressed in body coordinates equals the vector sum of velocity components expressed in world coordinates, an equivalent relationship does not hold for body and world acceleration vectors because the body coordinate frame is rotating. Specifically, differentiating Equation (6.22) with respect to time yields:

$$\frac{d}{dt}[V]_{world} = \frac{d}{dt}\left[\begin{array}{c|c} [R] & 0 \\ \hline 0 & [T] \end{array}\right][V]_{body} + \left[\begin{array}{c|c} [R] & 0 \\ \hline 0 & [T] \end{array}\right]\frac{d}{dt}[V]_{body} \quad \textbf{(6.26)}$$

Substituting acceleration [***A***] for time rate of change of [***V***] (as always in the appropriate coordinate frames) results in

$$[A]_{world} = \frac{d}{dt}\left[\begin{array}{c|c} [R] & 0 \\ \hline 0 & [T] \end{array}\right][V]_{body} + \left[\begin{array}{c|c} [R] & 0 \\ \hline 0 & [T] \end{array}\right][A]_{body} \quad \textbf{(6.27)}$$

Inspection of Equation (6.27) makes it clear that world coordinate frame accelerations $[A]_{world}$ and rotated body coordinate frame accelerations $[A]_{body}$ are not equivalent unless the transformation matrix between coordinate frames is unchanging, or all body velocities are zero (Greenwood 88). It is possible to examine accelerations acting upon the body from a perspective within the rotating body coordinate frame, but they cannot be directly integrated into world coordinate frame accelerations.

It is possible to numerically integrate the six dynamics equations with respect to time and determine new velocity values. This dynamics equation integration must be performed using body coordinate frame variables. Once new values for body velocities are thereby obtained, the six Euler kinematic constraint equations of motion (6.22) are utilized to produce linear and angular world velocities. Finally posture is determined within the world coordinate system using world velocities.

4. Time Dependencies

During operation of a vehicle in a virtual world, forces acting on the robot can be estimated from the vehicle state vector while velocities and body accelerations are analytically derived. During operation in the real world, forces can be similarly estimated while accurate velocity and body acceleration information may (or may not) be available from flow and inertial navigation sensors. In either world, good estimates of changes in body frame velocities are a primary robot requirement so that velocity and posture estimates can be cumulatively integrated over time. Accurately estimating body frame velocity changes at suitably short time intervals is the key to properly

modeling vehicle hydrodynamics response. Thus the dynamics equations of motion must be written to produce time rates of change of velocities as the dependent variables, obtained through calculations that solely involve vehicle variables (such as posture, propellers, thrusters and plane surfaces) which are continuously known to the robot.

The Newton-Euler formulation of Newton's Second Law from Equation (6.24) can be expanded by the chain rule to produce

$$[F]_{body} = \frac{d}{dt}\left([M]_{body} \cdot [V]_{body}\right) = \frac{d[M]}{dt}[V] + [M]\frac{d[V]}{dt} \qquad \textbf{(6.28)}$$

Within the body coordinate frame the mass matrix **[*M*]** is unchanging. Differentiation of the velocity matrix **[*V*]** reveals effects that are due to the body coordinate frame rotating with angular velocity ω with respect to the world coordinate frame (Fossen 94):

$$[F]_{body} = [M]\left([\dot{V}]_{body} + \omega \times [V]_{body}\right) \qquad \textbf{(6.29)}$$

Since matrix multiplication is associative but not commutative, both sides of matrix Equation (6.29) can be multiplied by a single matrix as long as order of multiplication is carefully preserved. In this case both sides of Equation (6.29) are multiplied by the mass matrix inverse $[\boldsymbol{M}]^{-1}$. Transposing the result yields Equation (6.30):

$$[\dot{V}]_{body} = [M]^{-1} \cdot [F]_{body} - \omega \times [V]_{body} \qquad \textbf{(6.30)}$$

This form of the dynamics equation is very important from a time-integration perspective, since all accelerations are grouped together on the left-hand side. All terms on the right-hand sides of the dynamics equations are known

or can be determined during vehicle operation in the virtual world. Thus calculation of the right-hand side can be used to determine updated values of the left-hand side.

Minimizing errors during the integration time step is essential for accurate real-time simulation of hydrodynamics models. This is due to the sensitivity of the hydrodynamics model to small perturbations, as well as the high degree of cross-coupling between forces acting on the three physical body axes of an submerged vehicle. If errors in determining body accelerations are minimized, then integration of body accelerations and subsequent coordinate frame transformations to yield velocities, positions and orientations will also minimize any accumulated errors inherent in velocity and posture estimation.

The local forces acting on an autonomous underwater vehicle are due to onboard effectors such as propellers, thrusters, planes and rudders. External ocean current forces are assumed to vary slowly with respect to vehicle time and act on the entire vehicle uniformly, having no effect on the interactions between the vehicle and the immediately adjacent water volume. Ocean current effects can therefore be added as a simple uniform translation. This vector addition is performed after fully calculating the effects of body accelerations and velocities, and after shifting back from a body coordinate system to the world coordinate system. Thus all forces can be completely determined or estimated in real time during vehicle operation. For constant-ballast vehicles, all elements of the body frame mass matrix [$\boldsymbol{M}$] and corresponding inverse [$\boldsymbol{M}$]$^{-1}$ can be determined empirically through prior testing (to a close first approximation) and are not time-varying.

5. Velocities and Postures

Combination of force and mass matrices as described above gives a very accurate estimation of time rates of change of body velocities. The body velocity rate matrix is integrated first to provide linear and rotational velocities, then integrated again to provide posture. Initial integration to yield body velocities occurs in the body fixed coordinate frame:

$$[V]_{body\ (t0+\delta t)} = \int_{t0}^{t0+\delta t} [\dot{V}]_{body\ (t)}\, dt + [V]_{body\ (t0)} \qquad \textbf{(6.31)}$$

Integration of the new body velocities to determine posture is preceded by a transformation from the body-fixed coordinate frame to the world coordinate frame. The following substitution pertains:

$$\int_{t0}^{t0+\delta t} [V]_{world\ (t)}\, dt = \int_{t0}^{t0+\delta t} \left([V]_{body\ (t)} \right)_{\substack{body \rightarrow world \\ coordinate\ shift}} dt \qquad \textbf{(6.32)}$$

The final integration to determine posture is therefore:

$$\begin{aligned} [Posture]_{world\ (t0+\delta t)} = & \int_{t0}^{t0+\delta t} [V]_{world\ (t)}\, dt \\ & + \int_{t0}^{t0+\delta t} [Ocean\ currents]_{world\ (t)}\, dt \\ & + [Posture]_{world\ (t0)} \end{aligned} \qquad \textbf{(6.33)}$$

6. Deriving Desired Form of Dynamics Equations of Motion

A full set of hydrodynamic equations of motion for a submerged vehicle are not usually written in the form suggested by Equations (6.30), (6.31), (6.32) and (6.33). Other derivations have been presented in the open literature (Gertler 76) (Smith 79) (Feldman 79) (Papoulias 89) (Watkinson 89) (Yuh 90) (Humphreys 91) (Baiardi 92) (Healey 93) (Fossen 94) and a variety of other sources, but are structured in such a way that similar time-dependent acceleration-related terms are present on both sides of the dynamics equations of motion. Because related body acceleration terms are not grouped together, direct time integration of both sides of the equations of motion is not mathematically valid in those representations. Furthermore these many references are all handicapped by variations in nomenclature and even a surprising variety of typographical errors, mathematical errors or omissions. None of these other models can be directly applied as a valid real-time underwater virtual

world component. *Therefore the primary intended contributions of the hydrodynamic model developed here are clarity, correctness, generality, standardized nomenclature and suitability for real-time simulation.*

Given this broad outline showing how the dynamics equations of motion will be utilized, it is time to derive the desired forms of the hydrodynamics equations. We can reorganize all of the original (Healey 93) equations of motion to solely have mass-related, inertia-related and $[\dot{V}]_{body}$-related terms on the left-hand side. That rearrangement leaves lift and drag, buoyancy, weight, propulsion thrust, and other forces and moments on the right-hand side. At any given instant t_0:

$$\begin{bmatrix} \boldsymbol{M} \\ \textit{mass, inertia} \\ \textit{and} \\ \textit{added-mass} \\ \textit{matrix} \end{bmatrix} \begin{bmatrix} \dot{u} \\ \dot{v} \\ \dot{w} \\ \dot{p} \\ \dot{q} \\ \dot{r} \end{bmatrix}_{(t_0)} = \begin{bmatrix} \textit{velocity-related} \\ \textit{inertial and} \\ \textit{hydrodynamic} \\ \textit{(drag and lift)} \\ \textit{force functions} \end{bmatrix}_{\left([V]_{body\,(t_0)}\right)} + \begin{bmatrix} \textit{buoyancy,} \\ \textit{weight,} \\ \textit{propulsion} \\ \textit{and other} \\ \textit{forces} \end{bmatrix}_{(t_0)} \quad \textbf{(6.34)}$$

Calculating the inverse mass matrix and multiplying it against both sides of Equation (6.34) leaves only body accelerations on the left-hand side. Further classification of individual terms on the right-hand side as corresponding to Coriolis, centripetal and other forces can be found in (Greenwood 88) (Healey 92c). For the purpose of this derivation it is sufficient to group these accelerations together without further discussion. Such an arrangement prepares the dynamics equations of motion for temporal integration in the body-fixed coordinate frame as follows:

$$\begin{bmatrix} \dot{u} \\ \dot{v} \\ \dot{w} \\ \dot{p} \\ \dot{q} \\ \dot{r} \end{bmatrix}_{(t_0)} = \begin{bmatrix} M^{-1} \\ mass\ matrix \\ inverse \end{bmatrix} \begin{bmatrix} dynamics \\ equations \\ of\ motion \\ right-hand \\ sides \end{bmatrix}_{(t_0)} \tag{6.35}$$

The body frame velocity matrix $[V]_{body}$ can now be updated by numerical integration. For example, Euler integration (Hamming 86) (Green 91) (Press 92) yields:

$$\begin{bmatrix} u \\ v \\ w \\ p \\ q \\ r \end{bmatrix}_{(t_0 + \delta t)} = \delta t \cdot \begin{bmatrix} \dot{u} \\ \dot{v} \\ \dot{w} \\ \dot{p} \\ \dot{q} \\ \dot{r} \end{bmatrix}_{(t_0)} + \begin{bmatrix} u \\ v \\ w \\ p \\ q \\ r \end{bmatrix}_{(t_0)} \tag{6.36}$$

A slightly more precise estimation of the velocity matrix can be achieved by averaging body acceleration at the beginning and end of each time step prior to integrating with respect to time. This method called second-order Runge-Kutta or *Heun* integration (Fossen 94), and is also the approach used for velocity estimation in the source code implementing this work (Brutzman 94e).

$$\begin{bmatrix} u \\ v \\ w \\ p \\ q \\ r \end{bmatrix}_{(t_0+\delta t)} = \delta t \cdot \frac{1}{2} \cdot \left(\begin{bmatrix} \dot{u} \\ \dot{v} \\ \dot{w} \\ \dot{p} \\ \dot{q} \\ \dot{r} \end{bmatrix}_{(t_0+\delta t)} + \begin{bmatrix} \dot{u} \\ \dot{v} \\ \dot{w} \\ \dot{p} \\ \dot{q} \\ \dot{r} \end{bmatrix}_{(t_0)} \right) + \begin{bmatrix} u \\ v \\ w \\ p \\ q \\ r \end{bmatrix}_{(t_0)} \quad \textbf{(6.37)}$$

where $[\dot{u}\ \dot{v}\ \dot{w}\ \dot{p}\ \dot{q}\ \dot{r}]^T_{(t+\delta t)}$ in Equation (6.37) is itself an estimate obtained by Euler integration of $[\dot{u}\ \dot{v}\ \dot{w}\ \dot{p}\ \dot{q}\ \dot{r}]^T_{(t)}$.

Conversion of these body velocities to world velocities is performed using the transformation of Equation (6.22). Subsequent integration of world velocities into world posture is performed by Euler integration as follows:

$$\begin{bmatrix} x \\ y \\ z \\ \phi \\ \theta \\ \psi \end{bmatrix}_{(t_0+\delta t)} = \delta t \cdot \begin{bmatrix} \dot{x} \\ \dot{y} \\ \dot{z} \\ \dot{\phi} \\ \dot{\theta} \\ \dot{\psi} \end{bmatrix}_{(t_0)} + \begin{bmatrix} x \\ y \\ z \\ \phi \\ \theta \\ \psi \end{bmatrix}_{(t_0)} \quad \textbf{(6.38)}$$

Final addition of ocean current effects completes the calculation of world coordinate system posture, as previously specified in Equation (6.33).

Increasingly accurate temporal resolution is possible using smaller time steps, chosen adaptively if necessary. Further numerical analysis considerations and recommendations appear in (Press 92) (Green 91) and (Hamming 86). In practice, a fixed time step of 0.1 seconds has worked well for model resolution, real-time robot hardware control response, network latency, remote interaction, computer graphics

rendering update rate, and human observation. Care must be taken if higher-order integration methods are employed to ensure that hydrodynamics model responsiveness does not degrade past the real-time requirements of the robot operating in the virtual world.

To summarize: the dynamics equations of motion are not mathematically rewritten in world coordinates, but are kept in body coordinates. Integrating the dynamics equations of motion provides body velocity values at the next time step. These new body coordinate frame velocities are combined with the kinematics equations of motion to produce world coordinate frame velocities. World velocities are then integrated and added to ocean current effects to produce updated world postures. Algorithmic complexity is sufficiently low to permit rapid model response within the same time period that the robot normally uses to query vehicle sensors.

7. Nomenclature Tables for Variables and Coefficients

The many details pertaining this approach still need to be filled in using a complete six-degree-of-freedom set of dynamics equations of motion. First, however, it must be noted that small yet persistent nomenclature inconsistencies were encountered in all of the dozens of hydrodynamics references studied. This is a serious problem for newcomers to the hydrodynamics literature, since both names and definitions of key terms may vary. This lack of standardization results in troubling mathematical incompatibilities throughout an entire body of scientific literature. Clearly an important prerequisite for describing any general hydrodynamics model is to use well-defined (and hopefully standardized) nomenclature. Of all the hydrodynamics models studied in this work, (Healey 93) and (Fossen 94) appear to be the most general and most applicable for real-time simulation of autonomous underwater vehicle response. The nomenclature of (Healey 93) closely follows that of the standard reference work on ship control (Lewis 88). The same nomenclature is followed here.

Since usage of a rigorously standardized nomenclature is only partially possible, this work will attempt to follow accepted conventions wherever possible

while precisely defining all variables and coefficients, both mathematically and descriptively. Coefficient subscripts from previous models have been corrected when necessary to explicitly indicate accompanying variable factors. Such an approach permits comparison of this hydrodynamics model with any other work, and hopefully provides clarity in a subject area that unfortunately includes wide variation.

The following tables define and describe the state variables and hydrodynamics coefficients used. Symbol, name, description, units and coefficient value (for the NPS AUV) are included. Variable and coefficient names in implementation software source code (Brutzman 94e) match exactly to further encourage clarity and correctness.

Close examination of the dynamics equations of motion reveals that nearly all of the hydrodynamics coefficients are dimensionless, having been normalized with respect to vehicle length $\boldsymbol{L}$. This convention permits rough comparison of the relative effects of individual coefficients with other vehicles or between different body axis orientations.

Coefficients presented here have been tested for a large variety of scenarios (Brutzman 94e). Nevertheless the complexities of hydrodynamics testing and intricacies of this model preclude complete validation, verification and accreditation. Constant coefficients are included for dynamics effects that occur in both cruise mode and hover mode. For vehicles that are capable of much higher speeds, coefficients are expected to become variable as a function of Reynolds Number, which quantifies the transition from laminar to fully developed turbulent fluid flow. Examination of Reynolds number effects on hydrodynamics coefficients appears in (Humphreys 89) (Ruth, Humphreys 90) (Humphreys 91). Further testing and refinement of hydrodynamics coefficients for various vehicles is an important subject for future work.

Although lengthy, proper definition of the numerous state variables and hydrodynamics coefficients is essential when producing and understanding a hydrodynamic model capable of providing precise response within an underwater

virtual world. The complete tables are presented here as an integral and essential part of the hydrodynamics model, in order to provide context for the derivations of the equations of motion which follow. A similarly exhaustive set of definitions for submarine simulation is included in (Feldman 79). NPS AUV II coefficient values are from (Warner 91) (Bahrke 92) (Marco 95) and laboratory testing. All angular definitions conform to the right-hand rule. Readers interested in comprehending the final six dynamics equations of motion are urged to closely examine the precise variable and coefficient definitions provided in these nomenclature tables.

Table 6.1. Hydrodynamics and Control System Variables.

Symbol	Name	Description	Coordinate system	Units
t	time	Clock time (real or simulated)	-	seconds
δt	time step	Loop interval (robot or dynamics model)	-	seconds
x	x	Position along North-South axis, North positive.	world	feet
y	y	Position along East-West axis, East positive.	world	feet
z	z	Depth, downward direction is positive.	world	feet
ϕ	roll Euler angle	Roll Euler angle rotation about North-South axis, preceding pitch and yaw rotations. Positive sense clockwise as seen from stern to bow of vehicle.	world	radians
θ	pitch Euler angle	Pitch Euler angle rotation about East-West axis, following rotation for roll and preceding rotation for yaw. Positive sense is clockwise as seen from port side of vehicle.	world	radians
ψ	yaw Euler angle	Yaw Euler angle rotation about vertical (depth) axis, following rotations for roll and pitch. Positive sense is clockwise as seen from above.	world	radians

Symbol	Name	Description	Coordinate system	Units
$\dot{x}$	x dot	Linear velocity along North-South axis.	world	ft/sec
$\dot{y}$	y dot	Linear velocity along East-West axis.	world	ft/sec
$\dot{z}$	z dot	Linear velocity along Depth axis.	world	ft/sec
$\dot{\phi}$	phi dot	Roll Euler angle rate component, about North-South axis. Not equivalent to ***p***.	world	radians/sec
$\dot{\theta}$	theta dot	Pitch Euler angle rate component, about East-West axis. Not equivalent to ***q***.	world	radians/sec
$\dot{\psi}$	psi dot	Yaw Euler angle rate component, about vertical (depth) axis. Not equivalent to ***r***.	world	radians/sec
u	surge	Linear velocity along longitudinal axis.	body	ft/sec
v	sway (sideslip)	Linear velocity along lateral axis.	body	ft/sec
w	heave	Linear velocity along vertical axis.	body	ft/sec
p	roll rate	Angular velocity component about longitudinal axis. Not equivalent to $\dot{\phi}$.	body	radians/sec
q	pitch rate	Angular velocity component about lateral axis. Not equivalent to $\dot{\theta}$.	body	radians/sec
r	yaw rate	Angular velocity component about vertical axis. Not equivalent to $\dot{\psi}$.	body	radians/sec

Symbol	Name	Description	Coordinate system	Units
$\dot{u}$	u dot	Time rate of change of surge velocity (along longitudinal axis)	body	ft/sec^2
$\dot{v}$	v dot	Time rate of change of sway velocity (along lateral axis)	body	ft/sec^2
$\dot{w}$	w dot	Time rate of change of heave velocity (along vertical axis)	body	ft/sec^2
$\dot{p}$	p dot	Time rate of change of roll angular velocity (about longitudinal axis)	body	radians/sec^2
$\dot{q}$	q dot	Time rate of change of pitch angular velocity (about lateral axis)	body	radians/sec^2
$\dot{r}$	r dot	Time rate of change of yaw angular velocity (about vertical axis)	body	radians/sec^2
δ_{rb}	bow rudders angle	Bow rudder deflection angle. Usually bow and stern rudders orders go to exactly opposite positions. Positive sense is clockwise as seen from above. Positive bow rudders angle with positive surge ***u*** produces positive change in yaw.	body	radians

Symbol	Name	Description	Coordinate system	Units
δ_{rs}	stern rudders angle	Stern rudder deflection angle. Usually bow and stern rudders go to exactly opposite positions). Positive sense is clockwise as seen from above. Positive stern rudders angle with positive surge ***u*** produces negative change in yaw.	body	radians
δ_{pb}	bow planes angle	Bow planes deflection angle. Usually bow and stern planes go to exactly opposite positions). Positive sense is clockwise as seen from the port side of the vehicle. Positive bow planes angle with positive surge ***u*** produces positive change in pitch.	body	radians
δ_{ps}	stern planes angle	Stern planes deflection angle. Usually bow and stern planeS go to exactly opposite positions). Positive sense is clockwIse as seen from the port side of the vehicle. Positive stern planes angle with positive surge ***u*** produces negative change in pitch.	body	radians
$\boldsymbol{n}_{porT}$	Port rpm	Port propeller ordered turns	body	rpm
$\boldsymbol{n}_{stbd}$	Stbd rpm	Starboard propeller ordered turns	body	rpm

Symbol	Name	Description	Coordinate system	Units
$V_{bow\text{-}vertical}$		Volts, bow vertical cross-body thruster (±24 V corresponds to ±2.0 lb)	body	volts
$V_{stern\text{-}vertical}$		Volts, stern vertical cross-body thruster (±24 V corresponds to ±2.0 lb)	body	volts
$V_{bow\text{-}lateral}$		Volts, bow lateral cross-body thruster (±24 V corresponds to ±2.0 lb)	body	volts
$V_{stern\text{-}lateral}$		Volts, stern lateral cross-body thruster (±24 V corresponds to ±2.0 lb)	body	volts

Table 6.2. Hydrodynamics Model Coefficients.

Coefficient	Name	Description	Value for NPS AUV II
W	weight	Submerged weight of vehicle, including water in contained free-flood spaces, neutral ballast.	435 lb
B	buoyancy	Weight of water displaced by vehicle, including water in contained free-flood spaces. Can vary with depth (due to hull compression) and with changes in water density ρ.	435 lb
L	length	Vehicle length, also known as characteristic length. Dynamics equations of motion are written to explicitly utilize L as a normalization coefficient. This approach makes most other coefficients dimensionless and quantitatively independent of vehicle dimensions, permitting comparison of relative effects between different forces and dissimilar vehicles.	7.302 ft
g		Acceleration due to gravity	32.174 ft/sec^2
ρ	rho	Mass density of fresh water: Mass density of sea water (representative):	1.94 slugs/ft^3 1.99 slugs/ft^3
m	mass	Vehicle mass, including water contained in enclosed free-flood spaces, neutral ballast.	W / g = 13.52 (lb· sec^2)/ft
I_x		Mass moment of inertia coefficient about body longitudinal axis, Equation (6.55)	2.7 ft·lb· sec^2

Coefficient	Name	Description	Value for NPS AUV II
I_y		Mass moment of inertia coefficient about body lateral axis, Equation (6.56)	42.0 ft·lb·sec^2
I_z		Mass moment of inertia coefficient about body vertical axis, Equation (6.57)	45.0 ft·lb·sec^2
I_{xy} $= I_{yx}$		Cross product of inertia coefficient, due to asymmetric mass distribution about body longitudinal/lateral axes, Equation (6.58)	0.0 ft·lb· sec^2
I_{xz} $= I_{zx}$		Cross product of inertia coefficient, due to asymmetric mass distribution about body longitudinal/vertical axes, Equation (6.59)	0.0 ft·lb· sec^2
I_{yz} $= I_{zy}$		Cross product of inertia coefficient, due to asymmetric mass distribution about body lateral/vertical axes, Equation (6.60)	0.0 ft·lb· sec^2
CG	center of gravity	Mass centroid of vehicle. The CG is the apparent point where forces and moments are applied.	(x_G, y_G, z_G)
x_G		Center of gravity location along body longitudinal axis, measured in body coordinates from nominal vehicle centroid	0.125 in = 0.010 ft
y_G		Center of gravity location along body lateral axis, measured in body coordinates from nominal vehicle centroid	0.0 ft

Coefficient	Name	Description	Value for NPS AUV II
z_G		Center of gravity location along body vertical axis, measured in body coordinates from nominal vehicle centroid. Note z_G is below center of buoyancy z_B by design for passive roll/pitch stability.	1.07 in = 0.089 ft
CB	center of buoyancy	Volumetric centroid of the vehicle.	(x_B, y_B, z_B)
x_B		Center of buoyancy location along body longitudinal axis	0.125 in = 0.010 ft
y_B		Center of buoyancy location along body lateral axis	0.0 ft
z_B		Center of buoyancy location along body vertical axis. Note z_B is above center of gravity z_G by design for passive roll/pitch stability.	0.0 ft
$x_{bow\text{-}vertical}$		Distance from nominal vehicle centroid to centerline of bow vertical thruster tunnel along body longitudinal axis.	1.41 ft
$x_{stern\text{-}vertical}$		Distance from nominal vehicle centroid to centerline of stern vertical thruster tunnel along body longitudinal axis. Note negative.	- 1.41 ft
$x_{bow\text{-}lateral}$		Distance from nominal vehicle centroid to centerline of bow lateral thruster tunnel along body longitudinal axis.	1.92 ft

Coefficient	Name	Description	Value for NPS AUV II
$x_{stern\text{-}lateral}$		Distance from nominal vehicle centroid to centerline of stern lateral thruster tunnel along body longitudinal axis. Note negative.	- 1.92 ft
$y_{port\text{-}propeller}$		Port propeller shaft offset from longitudinal centerline of vehicle	- 3.75 in = - 0.313 ft
$y_{stbd\text{-}propeller}$		Starboard propeller shaft offset from longitudinal centerline of vehicle	3.75 in = 0.313 ft
$h\ (x)$		Width of vehicle at body center along the y-axis, at a given position x measured on the longitudinal body axis	vehicle geometry tabular data
$b\ (x)$		Height of vehicle at body center along the z-axis, at a given position x measured on the longitudinal body axis	vehicle geometry tabular data
$U_{cf}\ (x)$		Total cross-flow velocity across body at a given body position x along longitudinal axis	see Equation (6.47)

Coefficient	Name	Description	Value for NPS AUV II
		Surge force coefficients	
	steady-state speed per maximum propeller rpm	Average forward velocity based on combined propeller revolutions per minute (rpm), typically measured at maximum steady-state speed. Analogous to turns-per-knot (TPK) ratio for ships with fixed-pitch propellers.	$\left(\frac{2 \text{ ft/sec}}{700 \text{ rpm}}\right)$ for twin propellers, steady state
X_{prop}		No longer used, since X_{prop} term is not a true coefficient. X_{prop} is now decomposed in Equation (6.43) to explicitly show individual contributing propulsion-related variables, which are then included in the revised surge equation of motion (6.48).	Not used. Previous values are no longer applicable.

Coefficient	Name	Description	Value for NPS AUV II
$X_{\dot{u}}$		Coefficients describing surge forces from resolved lift, drag and fluid inertia along body longitudinal axis. These occur in response to individual (or multiple) velocity, acceleration and plane surface components, as indicated by the corresponding subscripts. For example: $X_{\dot{u}}$ describes the drag contribution in the longitudinal ***X*** direction due to time rate of change of surge velocity ($\dot{u}$) Note that any coefficient may be non-zero, depending principally on the geometry of the vehicle being modeled.	-2.82 E-3
$X_{\dot{v}}$			0.0
$X_{\dot{w}}$			0.0
$X_{\dot{p}}$			0.0
$X_{\dot{q}}$			0.0
$X_{\dot{r}}$			0.0
X_{uu}			0.0
X_{vv}			0.0
X_{ww}			0.0
X_{pp}			0.0
X_{qq}			0.0
X_{rr}			0.0
$X_{uq\delta b}$			0.0
$X_{uq\delta s}$			0.0
$X_{ur\delta r}$			0.0
$X_{uv\delta r}$			0.0
$X_{uw\delta b}$			0.0
$X_{uw\delta s}$			0.0

Coefficient	Name	Description	Value for NPS AUV II
$X_{u\|u\|\delta b\delta b}$		Drag force due to square of deflection angle of bow planes (δ_{pb}), stern planes (δ_{ps}) and rudders (δ_{rb}, δ_{rs}) respectively due to square of surge ***u***	-1.018 E-2
$X_{u\|u\|\delta s\delta s}$			-1.018 E-2
$X_{u\|u\|\delta r\delta r}$			-1.018 E-2
X_{pr}		Fluid inertia force due to paired interactions as indicated by subscripted velocities, typically nonzero only as a result of asymmetries in the vehicle hull form	0.0
X_{wq}			0.0
X_{vp}			0.0
X_{vr}			0.0
C_{d0}		Drag coefficient along body longitudinal axis	0.00778
Note: for remaining coefficients, only non-negligible NPS AUV values are listed.			
Sway force coefficients			
$Y_{\dot{v}}$		Coefficients describing sway forces from resolved lift, drag and fluid inertia along body lateral axis. These occur in response to individual (or multiple) velocity, acceleration and plane surface components, as indicated by the corresponding subscripts.	-3.43 E-2
$Y_{\dot{r}}$			-1.78 E-1
Y_{uv}			-1.07 E-1
Y_{ur}			0.0
$Y_{u\|u\|\delta rb}$			+1.18 E-2
$Y_{u\|u\|\delta rs}$			+1.18 E-2
C_{dy}		Drag coefficient along body lateral axis	0.5

Coefficient	Name	Description	Value for NPS AUV II
Heave force coefficients			
$Z_{\dot{w}}$		Coefficients describing heave forces from resolved lift, drag and fluid inertia along body vertical axis. These occur in response to individual (or multiple) velocity, acceleration and plane surface components, as indicated by the corresponding subscripts.	-9.43 E-2
$Z_{\dot{q}}$			-2.53 E-3
Z_{uw}			-7.844 E-1
Z_{uq}			-7.013 E-2
$Z_{u\|u\|\delta pb}$			-2.11 E-2
$Z_{u\|u\|\delta ps}$			-2.11 E-2
C_{dy}		Drag coefficient along body vertical axis	0.6
Roll moment coefficients			
$K_{\dot{p}}$		Fluid inertia moment about longitudinal body axis due to time rate of change of roll rate ($\dot{p}$)	-2.4 E-4
$K_{\|u\|p}$		Fluid inertia moment about longitudinal body axis due to existing roll ***p*** and magnitude of surge ***u***	-5.4 E-3
$K_{p\|p\|}$		Drag moment about longitudinal body axis due to signed square of existing roll ***p*** corresponding to turbulent flow	-2.02 E-2 estimate

Coefficient	Name	Description	Value for NPS AUV II
K_p		Drag moment about longitudinal body axis due to existing roll ***p*** corresponding to laminar flow, approximately equals $K_{p\|p\|}$ at 1°/sec	$K_{p\|p\|}\left(\frac{\pi}{180°}\right)$ estimate
Pitch moment coefficients			
$M_{\dot{w}}$		Fluid inertia moment about lateral body axis due to time rate of change of heave rate ($\dot{w}$)	-2.53 E-3
$M_{\dot{q}}$		Fluid inertia moment about lateral body axis due to time rate of change of pitch rate ($\dot{q}$)	-6.25 E-3
M_{uw}		Fluid inertia moment about lateral body axis due to existing heave ***w*** and surge ***u***	0.0
M_{uq}		Fluid inertia moment about lateral body axis due to existing pitch ***q*** and surge ***u***	-1.53 E-2
$M_{u\|u\|\delta pb}$		Drag moment force about lateral body axis due to bow plane deflection δ_{pb} and signed square of surge ***u***	-0.283·L·$Z_{u\|u\|\delta pb}$
$M_{u\|u\|\delta ps}$		Drag moment about lateral body axis due to stern plane deflection δ_{ps} and signed square of surge ***u***	+0.377·L·$Z_{u\|u\|\delta ps}$
$M_{q\|q\|}$		Drag moment about lateral body axis due to signed square of existing pitch ***q*** corresponding to turbulent flow	-7.0 E-3 estimate

Coefficient	Name	Description	Value for NPS AUV II
M_q		Drag moment about lateral body axis due to existing pitch ***q*** corresponding to laminar flow, approximately equals $M_{q\|q\|}$ at 1°/sec	$M_{q\|q\|}\left(\frac{\pi}{180°}\right)$ estimate
Yaw moment coefficients			
$N_{\dot{v}}$		Fluid inertia moment about vertical body axis due to time rate of change of sway ($\dot{v}$)	-1.78 E-3
$N_{\dot{r}}$		Fluid inertia moment about vertical body axis due to time rate of change of yaw ($\dot{r}$)	-4.7 E-4
N_{uv}		Fluid inertia moment about vertical body axis due to existing sway ***v*** and surge ***u***	0.0
N_{ur}		Fluid inertia moment about vertical body axis due to existing yaw ***r*** and surge ***u***	-3.90 E-3
$N_{u\|u\|\delta rb}$		Drag moment about vertical body axis due to bow rudder deflection δ_{bs} and signed square of surge ***u***	$+0.283 \cdot L \cdot Y_{u\|u\|\delta rb}$
$N_{u\|u\|\delta rs}$		Drag moment about vertical body axis due to stern rudder deflection δ_{rs} and signed square of surge ***u***	$+0.377 \cdot L \cdot Y_{u\|u\|\delta rs}$
$N_{r\|r\|}$		Drag moment about vertical body axis due to signed square of existing yaw ***r*** corresponding to turbulent flow	-5.48 E-3 estimate

Coefficient	Name	Description	Value for NPS AUV II
N_r		Drag moment about vertical body axis due to existing yaw ***r*** corresponding to laminar flow, approximately equals $N_{r\|r\|}$ at 1°/sec	$N_{r\|r\|}\left(\frac{\pi}{180°}\right)$ estimate
N_{prop}		Propeller yaw moment for NPS AUV II is normally zero due to twin propellers that are identically paired, offsetting and counterrotating. However N_{prop} yaw moments are not zero if paired propeller rpm values differ. Actual moments equal $(F_{propeller} \cdot y_{propeller})$ for each propeller, now included in yaw equation of motion **(6.53)**.	Not used. Previous values are no longer applicable.

8. Modifications to Previous Dynamics Equations of Motion

Given these nomenclature definitions, the next task is to modify the dynamics equations of motion to group only body-acceleration-related terms on the left-hand sides, and group velocity-related terms on the right-hand sides. The algebraic transformations are similar for each of the six equations of motion. However the surge equation requires a number of important modifications and will be derived in detail. The surge equation describes the relationships between all forces affecting the linear body acceleration of the vehicle along the body longitudinal axis. The original surge motion equation of (Healey 93, appendix) includes accelerations on both sides and appears as follows:

Previous Surge Equation of Motion **(6.39)**

$$
\begin{aligned}
m\ [\dot{u} - vr + wq - x_G(q^2+r^2) + y_G(pq-\dot{r}) + z_G(pr+\dot{q})] \\
= \frac{\rho}{2}L^4\ [X_{pp}p^2+X_{qq}q^2+X_{rr}r^2+X_{pr}pr] \\
+ \frac{\rho}{2}L^3\ [X_{\dot{u}}\dot{u}+X_{wq}wq+X_{vp}vp+X_{vr}vr \\
+uq(X_{q\delta s}\delta_s+X_{q\delta b/2}\delta_{bp}+X_{q\delta b/2}\delta_{bs}+X_{r\delta r}ur\delta_r)+X_{r\delta_r}ur\delta_r] \\
+ \frac{\rho}{2}L^2\ [X_{vv}v^2+X_{ww}w^2+X_{V\delta r}uv\delta_r + uw(X_{w\delta s}\delta_s+X_{w\delta b/2}\delta_{bs}+X_{w\delta b/2}\delta_{bp}) \\
+ u^2(X_{\delta s\delta s}\delta_s^2+X_{\delta b\delta b/2}\delta_{\delta b}^2+X_{\delta r\delta r}\delta_r^2)] \\
+ (W-B)\sin\theta \\
+ \frac{\rho}{2}L^3\ X_{q\delta sn}uq\delta_s\epsilon(\eta) + \frac{\rho}{2}L^2\ [X_{w\delta sn}uw\delta_{sn}+X_{\delta s\delta sn}u^2\delta_s^2]\cdot\epsilon(\eta) \\
+ \frac{\rho}{2}L^2\ u^2X_{prop}
\end{aligned}
$$

The (Healey 93) equations of motion described and extended the earlier U.S. Navy Swimmer Delivery Vehicle hull number 9 (SDV-9) equations of motion (Smith 78, declassified), which were determined both empirically and theoretically. The $\varepsilon(\eta)$ term in Equation (6.39) approximates a second-order speed-related SDV-9

propulsion response as observed in tow tank testing. Tow tank testing is atypical for most underwater vehicles. Similarly, $\delta_{b/2}$ terms are related to an nonstandard control arrangement in the SDV-9 that included independent control of port and starboard bow planes. A split bow planes control configuration is not unusual, but more often plane surfaces are controlled in pairs. The effects of individual planes have been combined as pairs in this model for simplicity. Therefore the $\varepsilon(\eta)$ and $\delta_{b/2}$ terms are not included in the general model derived here.

Despite these reasonable simplifications it is worth noting that many existing underwater vehicles have asymmetries and unique characteristics which may not be fully captured by these general dynamics equations of motion. Additional modifications to the equations of motion may be necessary in some applications for proper characterization of different vehicle designs (such as individually controlled bow planes). For example, individual control of plane surface pairs will be necessary if active control of vehicle roll during cruise mode is attempted.

$\boldsymbol{X_{prop}}$ as defined in the original surge equation of motion of (Healey 93) composes a number of important variables including commanded speed, actual speed and drag. The $\boldsymbol{X_{prop}}$ formulation is not intuitive from the perspective of a general description of forces. Furthermore the composition of several variables as an apparent constant is very misleading. The following derivation algebraically reveals and rearranges the component variables making up the $\boldsymbol{X_{prop}}$ term. This reformulation permits distinguishing between propulsive force and drag force contributions occurring along the body longitudinal direction. Again from (Healey 93):

$$X_{prop} = C_{d0}(\eta|\eta| - 1) \tag{6.40}$$

$$\eta = \left(\frac{2\,ft/\sec}{700\,rpm}\right)\frac{n}{u} \tag{6.41}$$

where $\left(\frac{2\,ft/\sec}{700\,rpm}\right)$ can be referred to as *steady-state speed per maximum propeller rpm* ratio.

Combining (6.40) with (6.41) and expanding the last complete term contained in the (Healey 93) surge equation (6.39):

$$\begin{aligned}
\frac{\rho}{2}L^2u^2X_{prop} &= \frac{\rho}{2}L^2u|u|C_{d0}\,(\eta|\eta|-1) \\
&= \frac{\rho}{2}L^2u|u|C_{d0}\left[\frac{2\,ft/\sec}{700\,rpm}\,\frac{n}{u}\cdot\frac{2\,ft/\sec}{700\,rpm}\,\frac{|n|}{|u|}-1\right] \\
&= \frac{\rho}{2}L^2C_{d0}\left[\left(\frac{2\,ft/\sec}{700\,rpm}\right)^2 n|n|\,\frac{u}{u}\,\frac{|u|}{|u|}-u|u|\right] \\
&= \frac{\rho}{2}L^2C_{d0}\left[\left(\frac{2\,ft/\sec}{700\,rpm}\right)^2 n|n|-u|u|\right]
\end{aligned} \qquad \textbf{(6.42)}$$

The propulsion contribution (due to propeller rpm ***n***) and opposing drag contribution (due to forward surge velocity ***u***) are now evident. When the vehicle has two propellers, a pair of forward forces contribute to the expected speed per rpm, and the preceding $\boldsymbol{X_{prop}}$ term shown in Equation (6.42) is expanded to become:

$$\frac{\rho}{2}L^2u^2X_{prop} = \frac{\rho}{2}L^2C_{d0}\left[\left(\frac{2\,ft/\sec}{700\,rpm}\right)^2\frac{1}{2}\left(n_{port}|n_{port}|+n_{stbd}|n_{stbd}|\right)-u|u|\right] \qquad \textbf{(6.43)}$$

Force from a single propeller out of a pair is as follows. Corresponding yaw moment contributions by each of the propellers have been added to the yaw Equation (6.53).

$$F_{\substack{single-propeller\\(out\ of\ a\ pair)}} = \frac{\rho}{2}L^2C_{d0}\left[\left(\frac{2\,ft/\sec}{700\,rpm}\right)^2\frac{1}{2}\left(n_{prop}|n_{prop}|\right)-u|u|\right] \qquad \textbf{(6.44)}$$

Examination of Equations (6.43) and (6.44) reveals that, as forward velocity ***u*** increases, the effective forward thrust due to propeller rpm ***n*** decreases according to

the expected signed square law, similar to a pump curve of shaft rpm versus pressure head. Note that these equations also accurately describe drag forces against forward motion when a moving vehicle's propellers are turned off. Extensive test tank experimental data is not needed for measuring this predominant relationship between propeller thrust and forward speed. A straightforward measurement of steady-state speed for maximum propeller rpm precisely quantifies this relationship.

Cross-body thruster propulsion terms have also been added to the dynamics equations of motion. Steady-state thruster force is closely proportional to the signed square of ordered motor voltage for the cross-body thrusters designed and constructed for the NPS AUV II (Cody 92) (Healey 94b). This signed square relationship between control voltage and effective thruster force is shown in Equation (6.45). The sign convention for thruster voltages is that positive voltage results in a force which pushes the vehicle in the positive direction of the body lateral or depth axes. More precise modeling of thruster nonlinearities and sinusoidal-exponential time response is possible using generalized tunnel thruster dynamics models (Cody 92) (Healey 94b) (Brown 93) (Belton 93) (Fossen 94). Dynamics-based models of thruster response must be used instead if thruster temporal response is significant. Similar results have been found for other thrusters that include thrust controller circuitry (Sagatun 91) (Marks 92). A nontemporal signed square voltage model was found to be reasonably accurate for the overall effects of the NPS AUV thrusters. Open loop test tank experiments can quantify installed thruster performance versus time with little difficulty.

Since an accurate force equation is available to model the four individual thrusters, force and moment terms can be added directly to the sway, heave, pitch and yaw equations of motion. Physical offsets of thruster centerline away from the vehicle centroid are multiplied against forces to obtain corresponding moments, as shown in Equation (6.46). Opposing moments due to forward and aft thrusters are accounted for by positive and negative thruster tube offset distances, respectively. This eliminates the need for the previous $\boldsymbol{N}_{prop}$ formulation.

$$F_{thruster} = \left(\frac{2.0\ lb}{24^2\ volts} \right) V_{thruster} |V_{thruster}| \quad \textbf{(6.45)}$$

$$Moment_{thruster} = \left(\frac{2.0\ lb}{24^2\ volts} \right) V_{thruster} |V_{thruster}| \cdot x_{\substack{offset \\ distance}} \quad \textbf{(6.46)}$$

The addition of thruster forces and moments is required to extend the (Healey 93) model to remain valid at low forward speeds (i.e. hovering mode). Corresponding damping moments must also be included to model the resistance of water against rotational motion in these directions. Previously existing drag terms each include surge ***u*** as a factor, and each approaches zero at the low forward speeds associated with hovering. Therefore new rotational damping drag terms must be included to account for skin friction, particularly at low speeds. $\boldsymbol{K_{pp}}$, $\boldsymbol{M_{qq}}$, and $\boldsymbol{N_{rr}}$ are coefficients for quadratic terms corresponding to turbulent boundary layer skin friction. $\boldsymbol{K_p}$, $\boldsymbol{M_q}$, and $\boldsymbol{N_r}$ are coefficients for linear terms corresponding to laminar boundary layer skin friction. As suggested by (Sagatun 91) (Fossen 94), all six of these skin friction damping terms have been added to rotational dynamics equations of motion (6.51) through (6.53) respectively. $\boldsymbol{K_{prop}}$ and $\boldsymbol{M_{prop}}$ terms are no longer needed, for reasons analogous to those presented for $\boldsymbol{N_{prop}}$ previously.

One additional function needed for the dynamics equations of motion is $\boldsymbol{U_{cf}}$, a normalizing quantity for cross-body fluid flow with respect to body distance ***x*** along the vehicle longitudinal axis. From (Healey 93):

$$U_{cf}(x) = \sqrt{(v + xr)^2 + (w - xq)^2} \quad \textbf{(6.47)}$$

Related functions ***h(x)*** and ***b(x)*** in Table 6.2 and the dynamics equations of motion are provided for the NPS AUV by a table of cross-sectional measurements (Marco 95).

This is an example of *strip theory* which divides the body of a submerged vehicle into multiple parallel strips, estimates hydrodynamic coefficients for damping and added mass over each strip, and then sums the contribution over each strip to produce overall coefficient estimates (Fossen 94). Alternative methods of calculating cross-body flow forces and moments appear in (Humphreys 91).

Some additional explanation is necessary for time-varying forces. So-called "added mass" forces are related to the resistance of the surrounding fluid to vehicle body acceleration. This physical behavior is predictable and reasonably intuitive: acceleration of the immediately adjacent water volume requires a corresponding force, and is thereby referred to as an "added mass" effect. These forces are only proportional to vehicle accelerations and not vehicle velocities. This characteristic of a rigid body interacting with a fluid medium helps to explain why the body frame mass matrix **[*M*]** (which corresponds to vehicle mass, moments of inertia and "added mass") is time invariant.

Replacement of the $\boldsymbol{X}_{prop}$ and similar terms, removal of the $\varepsilon(\eta)$ and $\delta_{b/2}$ terms, including added mass terms, standardizing explicit nomenclature for hydrodynamics coefficients, and grouping body accelerations on the opposite sides from velocities now produces the desired form of the surge equation. Transformation of the remaining five equations of motion for sway, heave, roll, pitch and yaw is similarly performed by direct algebraic manipulation from those versions presented in (Healey 93). Thruster forces, thruster moments, propeller yaw moments and damping drag moments have been added where appropriate.

9. Dynamics Equations of Motion

The critical contribution of this chapter is the unambiguous definition of variables and coefficients, and a revised set of underwater vehicle dynamics equations of motion. These equations and the accompanying hydrodynamics model are implemented verbatim in the accompanying virtual world source code (Brutzman 94e). Final and complete forms for all six dynamics equations of motion follow.

Surge Equation of Motion (6.48)

$$\left(m - \frac{\rho}{2}L^3 X_{\dot{u}}\right)\dot{u} + m z_G \dot{q} - m y_G \dot{r}$$

$$= m\left[vr - wq + x_G(q^2 + r^2) - y_G pq - z_G pr\right]$$

$$+ \frac{\rho}{2}L^4\left[X_{pp}p^2 + X_{qq}q^2 + X_{rr}r^2 + X_{pr}pr\right]$$

$$+ \frac{\rho}{2}L^3\left[\begin{array}{l} X_{wq}wq + X_{vp}vp + X_{vr}vr + uq\left(X_{uq\delta b}\delta_{pb} + X_{uq\delta s}\delta_{ps}\right) \\ \qquad + ur\left(X_{ur\delta r}\delta_{rb} + X_{ur\delta r}\delta_{rs}\right)\end{array}\right]$$

$$+ \frac{\rho}{2}L^2\left[\begin{array}{l} X_{vv}v^2 + X_{ww}w^2 + uv\,X_{uv\delta r}\delta_{rs} + uw\left(X_{uw\delta b}\delta_{pb} + X_{uw\delta s}\delta_{ps}\right) \\ + u|u|\left(X_{u|u|\delta b\delta b}\delta_{pb}^2 + X_{u|u|\delta s\delta s}\delta_{ps}^2 + X_{u|u|\delta r\delta r}\delta_{rb}^2 + X_{u|u|\delta r\delta r}\delta_{rs}^2\right)\end{array}\right]$$

$$- (W - B)\sin(\theta)$$

$$+ \frac{\rho}{2}L^2 C_{d0}\left[\left(\frac{2\,ft/\sec}{700\,rpm}\right)^2 \frac{1}{2}\left(n_{port}|n_{port}| + n_{stbd}|n_{stbd}|\right) - u|u|\right]$$

Sway Equation of Motion (6.49)

$$\left(m - \frac{\rho}{2}L^3 Y_{\dot{v}}\right)\dot{v} + \left(-m z_G - \frac{\rho}{2}L^4 Y_{\dot{p}}\right)\dot{p} + \left(m x_G - \frac{\rho}{2}L^4 Y_{\dot{r}}\right)\dot{r}$$

$$= m\left[-ur + wp - x_G pq + y_G(p^2 + r^2) - z_G qr\right]$$

$$+ \frac{\rho}{2}L^4\left[Y_{pq}pq + Y_{qr}qr\right]$$

$$+ \frac{\rho}{2}L^3\left[Y_{up}up + Y_{ur}ur + Y_{vq}vq + Y_{wp}wp + Y_{wr}wr\right]$$

$$+ \frac{\rho}{2}L^2\left[Y_{uv}uv + Y_{vw}vw + u|u|\left(Y_{u|u|\delta rb}\delta_{rb} + Y_{u|u|\delta rs}\delta_{rs}\right)\right]$$

$$- \frac{\rho}{2}\int_{x\ tail}^{x\ nose}\left[C_{dy}\,h(x)\,(v + xr)^2 + C_{dz}\,b(x)\,(w - xq)^2\right]\frac{(v + xr)}{U_{cf}(x)}\,dx$$

$$+ (W - B)\cos(\theta)\sin(\phi)$$

$$+ \left(\frac{2\,lb}{24^2\,volts}\right)\left[V_{bow-lateral}|V_{bow-lateral}| + V_{stern-lateral}|V_{stern-lateral}|\right]$$

Heave Equation of Motion (6.50)

$$\left(m - \frac{\rho}{2}L^3 Z_{\dot{w}}\right)\dot{w} + m y_G \dot{p} + \left(-m x_G - \frac{\rho}{2}L^4 Z_{\dot{q}}\right)\dot{q}$$

$$= m\left[uq - vp - x_G pr - y_G qr + z_G(p^2 + q^2)\right]$$

$$+ \frac{\rho}{2}L^4\left[Z_{pp}p^2 + Z_{pr}pr + Z_{rr}r^2|\right]$$

$$+ \frac{\rho}{2}L^3\left[Z_{uq}uq + Z_{vp}vp + Z_{vr}vr\right]$$

$$+ \frac{\rho}{2}L^2\left[Z_{uw}uw + Z_{vv}v^2 + u|u|\left(Z_{u|u|\delta b}\delta_{pb} + Z_{u|u|\delta s}\delta_{ps}\right)\right]$$

$$- \frac{\rho}{2}\int_{x\ tail}^{x\ nose}\left[C_{dy}h(x)(v + xr)^2 + C_{dz}b(x)(w - xq)^2\right]\frac{(w - xq)}{U_{cf}(x)}dx$$

$$+ (W - B)\cos(\theta)\cos(\phi)$$

$$- \left(\frac{2\ lb}{24^2\ volts}\right)\left[V_{bow-vertical}|V_{bow-vertical}| + V_{stern-vertical}|V_{stern-vertical}|\right]$$

Roll Equation of Motion (6.51)

$$\left(m z_g - \frac{\rho}{2}L^4 K_{\dot{v}}\right)\dot{v} + m y_G \dot{w} + \left(I_x - \frac{\rho}{2}L^5 K_{\dot{p}}\right)\dot{p} - I_{xy}\dot{q} + \left(-I_{xz} - \frac{\rho}{2}L^5 K_{\dot{r}}\right)\dot{r}$$

$$= \left[-(I_z - I_y)qr - I_{xy}pr + I_{yz}(q^2 - r^2) + I_{xz}pq\right]$$

$$- m\left[y_G(-uq + vp) - z_G(ur - wp)\right]$$

$$+ \frac{\rho}{2}L^5\left[K_{pq}pq + K_{qr}qr + K_{p|p|}p|p| + K_p p\right]$$

$$+ \frac{\rho}{2}L^4\left[K_{|u|}p|u|p + K_{ur}ur + K_{vq}vq + K_{wp}wp + K_{wr}wr\right]$$

$$+ \frac{\rho}{2}L^3\left[K_{uv}uv + K_{vw}vw - u|u|\left(K_{u|u|\delta b}\delta_{pb} + K_{u|u|\delta s}\delta_{ps}\right)\right]$$

$$+ (y_G W - y_B B)\cos(\theta)\cos(\phi) - (z_G W - z_B B)\cos(\theta)\sin(\phi)$$

Pitch Equation of Motion (6.52)

$$
\begin{aligned}
& m z_G \dot{u} + \left(-m x_g - \frac{\rho}{2} L^4 M_{\dot{w}}\right)\dot{w} + -I_{xy}\dot{p} + \left(I_y - \frac{\rho}{2} L^5 M_{\dot{q}}\right)\dot{q} - I_{yz}\dot{r} \\
&= \left[-(I_x - I_z)pr + I_{xy}qr - I_{yz}pq - I_{xz}(p^2 - r^2)\right] \\
&\quad + m\left[x_G(-uq + vp) - z_G(-vr + wq)\right] \\
&\quad + \frac{\rho}{2} L^5\left[M_{pp}p^2 + M_{pr}pr + M_{r|r|}\, r\,|r| + M_{q|q|}\, q\,|q| + M_q q\right] \\
&\quad + \frac{\rho}{2} L^4\left[M_{uq}\, uq + M_{vp}\, vp + M_{vr}\, vr\right] \\
&\quad + \frac{\rho}{2} L^3\left[M_{uw}\, uw + M_{vv}\, v^2 + u\,|u|\left(M_{u|u|\,\delta b}\delta_{pb} + M_{u|u|\,\delta s}\delta_{ps}\right)\right] \\
&\quad + \frac{\rho}{2}\int_{x\ tail}^{x\ nose}\left[C_{dy}\, h(x)\,(v + xr)^2 + C_{dz}\, b(x)\,(w - xq)^2\right]\frac{(w - xq)}{U_{cf}(x)}\, x\, dx \\
&\quad - (x_G W - x_B B)\cos(\theta)\cos(\phi) - (z_G W - z_B B)\sin(\theta) \\
&\quad - \left(\frac{2\ lb}{24^2\ volts}\right)\begin{bmatrix} V_{bow-vertical}\,|V_{bow-vertical}|\cdot x_{bow-vertical} + \\ V_{stern-vertical}\,|V_{stern-vertical}|\cdot x_{stern-vertical} \end{bmatrix}
\end{aligned}
$$

Yaw Equation of Motion (6.53)

$$
\begin{aligned}
m y_G \dot{u} + \left(m x_g - \frac{\rho}{2} L^4 N_{\dot{v}} \right) \dot{v} + \left(-I_{xz} - \frac{\rho}{2} L^5 N_{\dot{p}} \right) \dot{p} + -I_{yz} \dot{q} + \left(I_z - \frac{\rho}{2} L^5 N_{\dot{r}} \right) \dot{r} \\
= \quad \left[-(I_y - I_x) pq + I_{xy}(p^2 - q^2) + I_{yz} pr - I_{xz} qr \right] \\
- m \left[x_G (ur - wp) - y_G (-vr + wq) \right] \\
+ \frac{\rho}{2} L^5 \left[N_{pq} pq + N_{qr} qr + N_{r|r|} r|r| + N_r r \right] \\
+ \frac{\rho}{2} L^4 \left[N_{up} up + N_{ur} ur + N_{vq} vq + N_{wp} wp + N_{wr} wr \right] \\
+ \frac{\rho}{2} L^3 \left[N_{uv} Uv + N_{vw} vw + u|u| \left(N_{u|u|\delta rb} \delta_{rb} - N_{u|u|\delta rs} \delta_{rs} \right) \right] \\
- \frac{\rho}{2} \int_{x\ tail}^{x\ nose} \left[C_{dy} h(x) (v + xr)^2 + C_{dz} b(x) (w - xq)^2 \right] \frac{(v + xr)}{U_{cf}(x)} x\, dx \\
+ (x_G W - x_B B) \cos(\theta) \sin(\phi) + (y_G W - y_B B) \sin(\theta) \\
+ \left(\frac{2\ lb}{24^2\ volts} \right) \begin{bmatrix} V_{bow-lateral} |V_{bow-lateral}| \cdot x_{bow-lateral} + \\ V_{stern-lateral} |V_{stern-lateral}| \cdot x_{stern-lateral} \end{bmatrix} \\
- F_{port-propeller} \cdot y_{port-propellor} - F_{stbd-propeller} \cdot y_{stbd-propeller}
\end{aligned}
$$

10. Mass and Inertia Matrix [M]

Matrix equations can now be written from the dynamics equations of motion (6.48) through (6.53), grouping significant terms together appropriately. The left-hand sides are simply written in matrix form as the product of the body coordinate frame mass matrix [***M***] and the time rate of change of velocities matrix $[\dot{V}]_{body}$. The force matrix [***F***] is a (6 × 1) matrix comprised of the right-hand sides of the six dynamics equations of motion.

The body coordinate frame mass matrix [***M***] is determined from the coefficients corresponding to linear and rotational components of $[\dot{V}]_{body}$ on the left-hand side of the given equations of motion **(6.48)** through **(6.53)**. When expressed properly, this mass matrix is time-invariant and does not include any velocity-related terms. All possible added mass terms are included here for completeness, even though many of the terms are likely to equal zero (Fossen 94).

Mass Matrix **(6.54)**

$$[M] = \begin{bmatrix} m-\frac{\rho}{2}L^3X_{\dot{u}} & -\frac{\rho}{2}L^3X_{\dot{v}} & -\frac{\rho}{2}L^3X_{\dot{w}} & -\frac{\rho}{2}L^4X_{\dot{p}} & mz_G-\frac{\rho}{2}L^4X_{\dot{q}} & -my_G-\frac{\rho}{2}L^4X_{\dot{r}} \\ -\frac{\rho}{2}L^3Y_{\dot{u}} & m-\frac{\rho}{2}L^3Y_{\dot{v}} & -\frac{\rho}{2}L^3Y_{\dot{w}} & -mz_G-\frac{\rho}{2}L^4Y_{\dot{p}} & -\frac{\rho}{2}L^4Y_{\dot{q}} & mx_G-\frac{\rho}{2}L^4Y_{\dot{r}} \\ -\frac{\rho}{2}L^3Z_{\dot{u}} & -\frac{\rho}{2}L^3Z_{\dot{v}} & m-\frac{\rho}{2}L^3Z_{\dot{w}} & my_G-\frac{\rho}{2}L^4Z_{\dot{p}} & -mx_G-\frac{\rho}{2}L^4Z_{\dot{q}} & -\frac{\rho}{2}L^4Z_{\dot{r}} \\ -\frac{\rho}{2}L^4K_{\dot{u}} & -mz_G-\frac{\rho}{2}L^4K_{\dot{v}} & my_G-\frac{\rho}{2}L^3K_{\dot{w}} & I_x-\frac{\rho}{2}L^5K_{\dot{p}} & -I_{xy}-\frac{\rho}{2}L^5K_{\dot{q}} & -I_{xz}-\frac{\rho}{2}L^5K_{\dot{r}} \\ mz_G-\frac{\rho}{2}L^4M_{\dot{u}} & -\frac{\rho}{2}L^4M_{\dot{v}} & -mx_G-\frac{\rho}{2}L^4M_{\dot{w}} & -I_{xy}-\frac{\rho}{2}L^5M_{\dot{p}} & I_y-\frac{\rho}{2}L^5M_{\dot{q}} & -I_{yz}-\frac{\rho}{2}L^5M_{\dot{r}} \\ -my_G-\frac{\rho}{2}L^4N_{\dot{u}} & mx_G-\frac{\rho}{2}L^4N_{\dot{v}} & -\frac{\rho}{2}L^4N_{\dot{w}} & -I_{xz}-\frac{\rho}{2}L^5N_{\dot{p}} & -I_{yz}-\frac{\rho}{2}L^5N_{\dot{q}} & I_z-\frac{\rho}{2}L^5N_{\dot{r}} \end{bmatrix}$$

The spatial distribution of mass within a body has several important effects which are quantified as moments of inertia. Calculation of inertial moments are as shown in Equations (6.55) through (6.60). In practice these calculations are performed as weighted sums, measured from vehicle origin to centers of mass for individual internal vehicle components. If the vehicle has a variable ballast system, changes of mass and inertial moment must be accounted for and then the body frame mass matrix **[*M*]** becomes slowly time-varying.

$$I_x = \int (y^2 + z^2)\, dm \tag{6.55}$$

$$I_y = \int (x^2 + z^2)\, dm \tag{6.56}$$

$$I_z = \int (x^2 + y^2)\, dm \tag{6.57}$$

$$I_{xy} = I_{yx} = \int x y\, dm \tag{6.58}$$

$$I_{xz} = I_{zx} = \int x z\, dm \tag{6.59}$$

$$I_{yz} = I_{zy} = \int y z\, dm \tag{6.60}$$

Mass matrix inversion can be accomplished via any of several algorithms (Press 92) (Hamming 86). Note that since the body frame mass matrix [***M***] is ordinarily time-invariant, the inverse mass matrix $[\boldsymbol{M}]^{-1}$ does not have to be determined repeatedly. Thus the computational efficiency of this large matrix inversion

calculation has no effect on the real-time responsiveness of the hydrodynamics model algorithm. If total vehicle mass or inertial moment changes due to variable ballast or significant moving internal components, the matrix inversion calculation will have to be occasionally repeated and may impact real-time response.

11. Summary of Hydrodynamics Model Algorithm

All of the components of the general underwater vehicle real-time hydrodynamics model have been presented. Figure 6.5 summarizes the hydrodynamics model algorithm.

- Estimate and invert mass matrix **[*M*]** using **equation (6.54)**
- Initialize hydrodynamics model variables for posture **[*P*]**, velocities **[*V*]** and time rates of change of velocities using **Table 6.1**
- Loop until robot is done:
  - receive updated state vector from robot, including ordered effector values for rudders, planes, propellers, thrusters and elapsed time
  - Calculate new values for time rate of change of body velocities, using the current vehicle state vector and equation of motion right-hand sides using **Table 6.2, equations (6.24), (6.30), (6.35), and (6.48) through (6.53)**
  - Update velocities $[V]_{body}$ using **equation (6.31)**
  - Perform transformation to $[V]_{world}$ using **equations (6.5), (6.9), (6.10), (6.11), and (6.22)**
  - Update posture **[*P*]** using newly-calculated velocities $[V]_{world}$, ocean current estimate and previous posture using **equation (6.33)**
  - Return newly-calculated hydrodynamics values to robot via telemetry update of the robot state vector. Most calculated velocities and accelerations correspond to real-world values provided by inertial, flow and pressure sensors.
  - Wait for next updated state robot vector. Continue loop upon receipt. Shutdown when model is no longer required by robot.

Figure 6.5. Underwater vehicle real-time hydrodynamics modeling algorithm.

E. EULER ANGLE METHODS COMPARED TO QUATERNION METHODS

The hydrodynamics model presented here is based on Euler angle representations of vehicle orientation. Another possible representation method of interest is the unit quaternion. The use of quaternions is most notable for a lack of singularity when pointing vertically, and also for well-developed mathematics that permits rapid and efficient orientation update rates (Cooke 92b) (Kolve 93) (Chou 92) (Funda 90) (Shoemake 85). This section briefly describes quaternion mathematics as a possible alternative to Euler angle orientation calculations in the underwater vehicle hydrodynamics model.

The underlying mathematical reason that an Euler angle rotation matrix is unable to satisfactorily represent a vehicle pointing vertically (along the ***z***-axis) is that extraction of Euler angles provides a unique value for pitch ($\theta = \pm\pi$) but can only provide the sum ($\phi + \psi$, nose up) or difference ($\phi + \psi$, nose down) of roll and yaw, not unique values for each. Thus three parameters are inadequate to unambiguously represent all possible orientations as desired. Sir William Rowan Hamilton deduced and developed quaternion algebra in 1843 after searching many years for a generalization of complex numbers. He determined that four parameters are necessary to represent all possible orientations without potential mathematical singularity (Cooke 92b).

Consider the unit sphere as illustrated in Figure 6.6. Three parameters are necessary to describe a unit vector directed from the center to any point on the sphere surface. A fourth parameter can then be used to describe a value for rotation about this axis. This combination of unit vector and axial rotation uniquely defines all possible orientations, provided rotation values are specified to have a range $[0..2\pi)$ (Euler's Theorem).

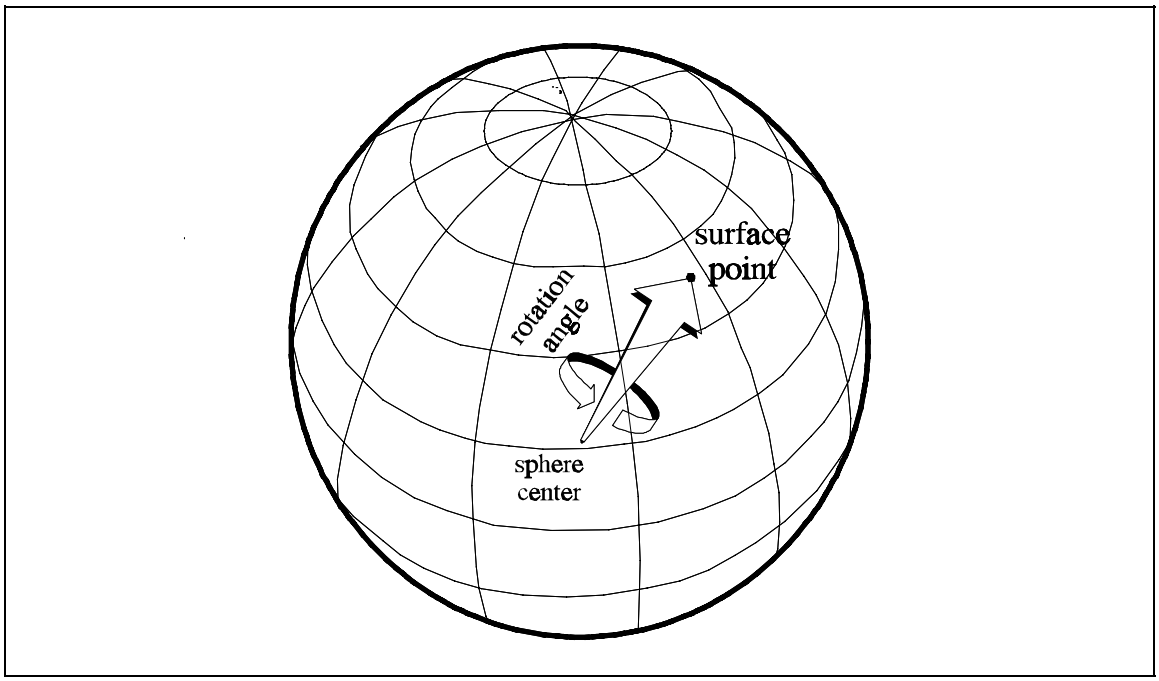

Figure 6.6. Quaternion representation.

There are several ways to represent quaternion values, described in detail in (Cooke 92a, 92b) (Kolve 93) (Chou 92) (Funda 90) (Maillot 90) and (Shoemake 85). The simplest representation is to scale three orthogonal unit vectors $\hat{i}$, $\hat{j}$, and $\hat{k}$ to indicate a point in three space, and then combine those three terms with another value for rotation about the described axis as follows:

$$Q = W + \hat{i}\,X + \hat{j}\,Y + \hat{k}\,Z \qquad \textbf{(6.61)}$$

The Euler parameter representation follows an Euler angle approach to state that three angles **A**, **B** and **C** can provide a rotation matrix that will align a rotation axis with the world coordinate frame. A fourth angle **D** describes rotation about this axis.

Rather than use **A**, **B**, **C** and **D** directly, a unit quaternion ***Q*** is represented using the following substitutions:

$$Q = \langle q_0,\ q_1,\ q_2,\ q_3 \rangle \tag{6.62}$$

where

$$\begin{aligned} q_0 &= \cos\left(\frac{D}{2}\right) \\ q_1 &= \cos(A)\ \sin\left(\frac{D}{2}\right) \\ q_2 &= \cos(B)\ \sin\left(\frac{D}{2}\right) \\ q_3 &= \cos(C)\ \sin\left(\frac{D}{2}\right) \end{aligned} \tag{6.63}$$

The four component values of quaternion ***Q*** are called *Euler parameters*. Expressing quaternions using Euler parameter form is desirable due to improved computational efficiency during arithmetic operations. Normalization may be periodically required after numerical calculations to ensure that magnitude of each unit quaternion vector remains equal to unity (Cooke 92b).

One important property of unit quaternions as described above is especially useful. Multiplication of two unit quaternions produces a new unit quaternion which represents the results of two successive corresponding rotations.

$$\begin{aligned} Q \cdot Q_1 &= \left(W + \hat{i}X + \hat{j}Y + \hat{k}Z\right)\left(W_1 + \hat{i}X_1 + \hat{j}Y_1 + \hat{k}Z_1\right) \\ &= \left(WW_1 - XX_1 - YY_1 - ZZ_1\right) \\ &\quad + \hat{i}\left(XW_1 + WX_1 - ZY_1 + YZ_1\right) \\ &\quad + \hat{j}\left(YW_1 + ZX_1 - WY_1 + XZ_1\right) \\ &\quad + \hat{k}\left(ZW_1 + YX_1 - XY_1 + WZ_1\right) \end{aligned} \tag{6.64}$$

Angular velocity of a rigid body can be converted from body coordinate frame angular velocities to quaternion rates as follows:

$$\begin{aligned} \dot{q}_0 &= -\tfrac{1}{2}\left(q_1 p + q_2 q + q_3 r\right) \\ \dot{q}_1 &= \tfrac{1}{2}\left(q_0 p + q_2 r - q_3 q\right) \\ \dot{q}_2 &= \tfrac{1}{2}\left(q_0 q + q_3 p - q_1 r\right) \\ \dot{q}_3 &= \tfrac{1}{2}\left(q_0 r + q_1 q - q_2 p\right) \end{aligned} \qquad \textbf{(6.65)}$$

Given an initial orientation represented by a quaternion ***Q***, orientation updates are obtained by periodically integrating quaternion ***Q*** using quaternion rate $\dot{Q}$ and time step (δt) via any numerical integration method.

Euler angles, if needed, are then extracted from the updated quaternion $Q_{(t_0 + \delta t)}$ as follows (Cooke 92b):

$$\theta = \sin^{-1}\left(-2\,(q_1 q_3 - q_0 q_2)\right) \qquad \textbf{(6.66)}$$

$$\psi = \cos^{-1}\left(\frac{q_0^2 + q_1^2 - q_2^2 - q_3^2}{\cos(\theta)}\right) \cdot \operatorname{sign}(q_1 q_2 + q_0 q_3) \qquad \textbf{(6.67)}$$

$$\phi = \cos^{-1}\left(\frac{q_0^2 - q_1^2 - q_2^2 + q_3^2}{\cos(\theta)}\right) \cdot \operatorname{sign}(q_2 q_3 + q_0 q_1) \qquad \textbf{(6.68)}$$

Note that the vertical restrictions on the range of pitch angle θ from Equation (6.2) remain unchanged in Equations (6.67) and (6.68) when converting from the quaternion representation back to Euler angles. Further mathematical manipulations of the quaternion will not produce values for ϕ or ψ. However, unlike

the singularity in Euler rates at $\theta = \pm \pi/2$, there is no corresponding singularity in the quaternion rates of Equation (6.65).

The principal drawback to using quaternions in an underwater virtual world hydrodynamics model is greater computational complexity when calculating Euler angles, which are needed for networked posture update reports. The principal advantage of quaternion arithmetic is that computational complexity is less than Euler angle methods when solely calculating rotational updates (Cooke 92b). In the current implementation of the virtual world, Euler angles are required at every time step, in order to produce sensor values in the vehicle state vector and in order to provide DIS network updates. Thus Euler angle methods are used in the hydrodynamics model implementation (Brutzman 94e). These requirements might change if another vehicle without sucH sensors were modeled. If no virtual vehicle yaw, pitch or roll sensors are being modeled, or if DIS network updates are infrequent, the periodic computational drawback of quaternion conversions to Euler angles might become negligible. The mathematical methodology presented in this section demonstrated how to utilize quaternions for recording and updating orientation rotations in the hydrodynamics model, as an alternative to Euler angle methods. Detailed comparisons of computational efficiency including network considerations appear in (Cooke 92a, 92b).

F. DISTRIBUTED INTERACTIVE SIMULATION (DIS) AND NETWORK CONSIDERATIONS

Distributed Interactive Simulation (DIS) is the IEEE standard protocol (IEEE 93) used for communicating between networked entities sharing the same virtual environment. In order for a robot operating in a virtual world to be visible to other entities, DIS Protocol Data Units (PDUs) are sent out at regular intervals. The purpose and implementation of the virtual world DIS interface are presented separately in the network considerations chapter. This section examines the specific requirements of the hydrodynamics model that pertain to DIS.

The purpose of the hydrodynamics model is to provide valid real-time response to a networked robot operating in a virtual world. The hydrodynamics model is complex and sophisticated. A wide variety of subtle physical responses are possible. One current focus of research interest is examining the precise interactions that occur between robot and hydrodynamics models. Fine-grained reproduction of every interaction is therefore desirable for scientific purposes, if supportable by the network and virtual world viewer programs. Reproduction of AUV state at the same rate as interactions between the robot and the hydrodynamics model is correspondingly useful for visualization of both robot vehicle performance and hydrodynamics model performance. Currently this interaction rate is ten times per second (10 Hz).

The DIS protocol requires that entities announce their position at intervals not to exceed 5 seconds so that other entities are aware of their "live" presence (IEEE 93). In practice an interval of one to three seconds is typically used for entities such as ground vehicles which usually move with constant linear velocity. Highly dynamic vehicles such as jet aircraft may announce posture data many times per second in order to permit smooth refresh rates of rapidly varying postures (Towers 94). In order to reduce unnecessary network traffic, adaptive time steps between PDUs are recommended which only broadcast new values when predicted dead-reckoning error exceeds a reasonable threshold (or when the 5 second keep-alive deadline is reached). Choice of dead reckoning algorithm and other parameters can also reduce network loading (Lin 94). In general, minimizing PDU traffic is important to reduce network bandwidth, and also to reduce the processing load on each DIS receiver. These bandwidth considerations grow in importance when the number of actively participating entities becomes large, and also when using multicast DIS which can have world-wide Internet scope (Macedonia, Brutzman 94).

Although linear and rotational velocities and accelerations of an underwater vehicle are orders of magnitude lower than jet aircraft, underwater vehicle behavior is highly dynamic nevertheless. Example missions demonstrating highly complex interrelationships among vehicle state variables appear in the experimental results

chapter and software distribution (Brutzman 94e). For some missions, frequent posture updates are necessary to closely evaluate vehicle interaction with hazardous environments in close quarters (such as a minefield). Precise posture information is also necessary to indicate interactions of propulsor flow and sonar sensors with the environment. Currently thrust, control plane and sonar values are embedded as "articulated parameters" within individual DIS entity state PDUs for the NPS AUV. Future versions of the DIS standard are expected to provide new PDU types specifically designed for announcing sonar transmissions, but hydrodynamics flow vectors (proportional to propulsor values) will continue to be inferred from the vehicle entity state PDU articulated parameter values.

Entity state PDUs must contain posture values and can optionally include linear velocity, angular velocity, and linear acceleration. Dead reckoning algorithm velocities and accelerations may be in world or body coordinates. Body accelerations are not explicitly defined, but (Towers 94) presents two dead reckoning algorithms pertaining to each of two possible body acceleration definitions. Of particular note are experimental results which show that average processing time of world coordinate frame PDUs is only 80% relative to body coordinate frame PDUs (Towers 94). On the other hand, a computational drawback in the use of world coordinate frame PDUs here is the fact that the underwater vehicle hydrodynamics model does not directly provide accelerations in the world coordinate frame. The current DIS implementation in the underwater virtual world utilizes world coordinate frame PDUs because they are more efficient for receivers and less expensive to render. Future work of interest includes implementing a selectable alternative encoding of entity state velocities and accelerations in body frame coordinates, and then empirically evaluating whether virtual world efficiency is degraded by shifting PDUs to body coordinates. Dead reckoning algorithm efficiency and evaluation is further discussed in (Lin 94).

G. OBJECT-ORIENTED NETWORKED RIGID BODY DYNAMICS CLASS HIERARCHY

Physically based modeling includes dynamics (modeling forces and accelerations) as well as kinematics (modeling velocity effects only). Dynamics considerations are a superset of kinematics. The implementation of the underwater vehicle hydrodynamics model was designed to incorporate the principles of object-oriented programming (encapsulation, inheritance and polymorphism) and structured programming (top-down design, modularity and data abstraction) as appropriate (Booch 91) (Barr 91) (Stroustrup 91) (Frakes 91) (Barzel 92) (Pohl 93) (Bailey 94). The many good design and software engineering principles found in these references were valuable in managing the complexity of the hydrodynamics model, and also in building a general dynamics model that can be easily adapted to other underwater vehicles (or even other vehicle types). Although no single software engineering methodology was rigidly adhered to, the resulting model implementation (written in ***C***++) enjoys most of the benefits which motivate these various references. Model structure is briefly presented here and further described in (Brutzman 94e).

Structuring the model design problem was the key to comprehensible implementation. A straightforward hierarchy follows. Posture is common to all vehicles and can be represented either by Euler angles, by Euler angles embedded in a homogenous transformation matrix (Fu 87) (Foley, van Dam 90), or by quaternions (Cooke 92b). A rigid body is subject to kinematics equations of motion which combine velocities with postures in strictly defined ways regardless of vehicle type or environmental dimensionality. A networked rigid body which communicates with other entities via DIS needs to calculate postures, optional linear and rotational velocities, and (again optional) linear accelerations. Such a DIS-networked rigid body has identical capabilities regardless of vehicle type. An entity dynamics component for a real-time networked virtual world combines the functionality of rigid bodies and DIS networking with the dynamics equations of motion (forces and accelerations) unique to a specific vehicle type. This structured hierarchy of relationships between

posture representations, rigid bodies, DIS networking and dynamics equations of motion led to the general model class diagram which appears in Figure 6.7.

The compartment boxes in Figure 6.7 delineate the functionality of class components. The first compartment is class name. The second compartment indicates member data fields, which are the data structures encapsulated by the object. The third compartment indicates object methods (functions) which effectively occur instantaneously. The fourth compartment includes methods (functions) which are time-consuming, either from the perspective of simulation clock duration or actual delay due to network latency. Adapted from the Object-Oriented Simulation Pictures (OOSPICs) design and testing methodology (Bailey 94), this diagraming approach is very useful because it simplifies presentation of key object relationships and clarifies hierarchy design. Of particularly value is the explicit specification of temporal relationships, which are critical to success in a real-time system and are often overlooked in complex system design. An example object template which adapts the OOSPICs methodology from ***MODSIM*** programming language to ***C***++ appears as Figure 6.8. A key for OOSPIC arrow conventions is included in Figure 6.9 (Bailey 94). Software source code throughout the hydrodynamics class library implementation (Brutzman 94e) follows the structural layout presented in the OOSPIC diagram of Figure 6.8.

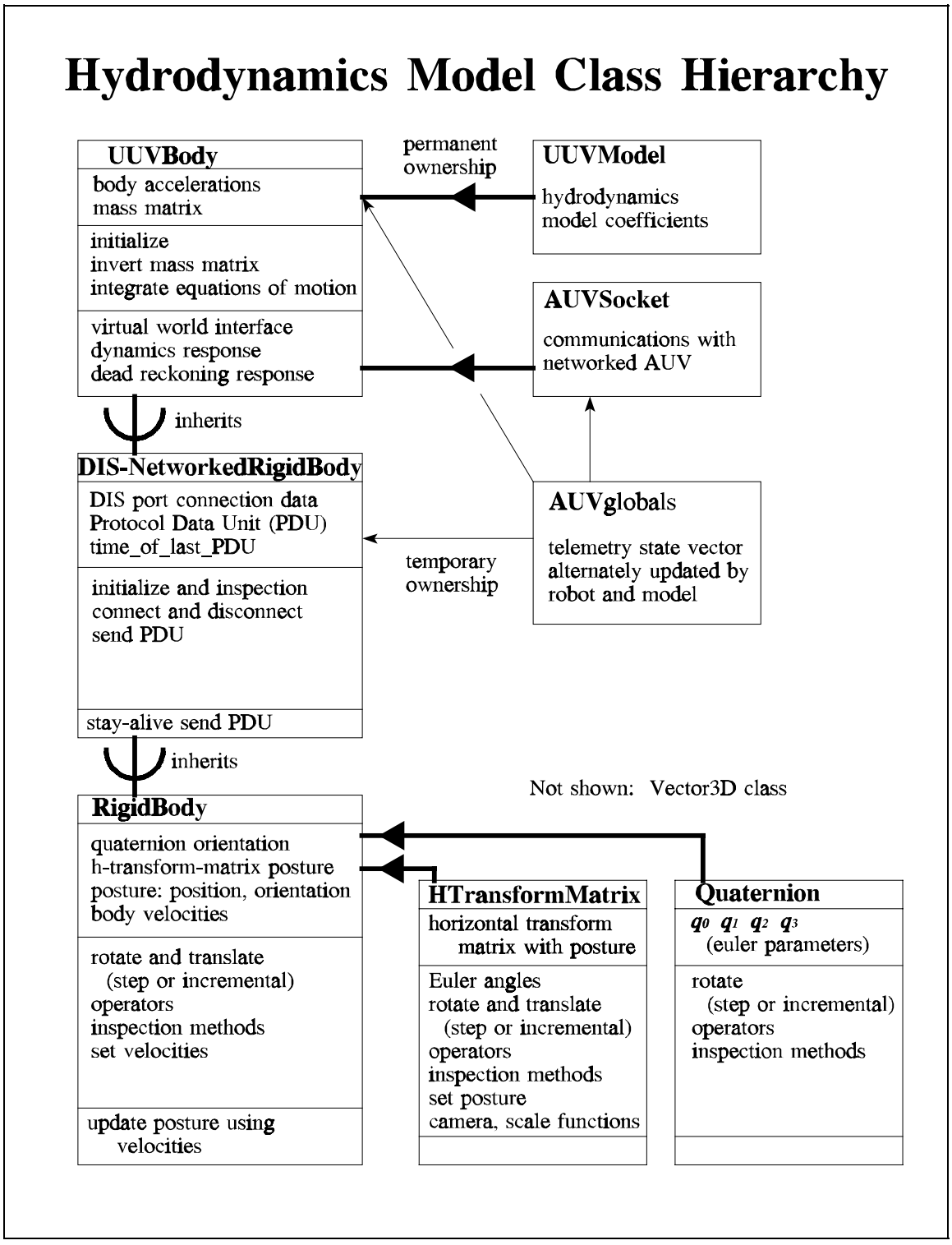

Figure 6.7. General real-time DIS-networked hydrodynamics model class hierarchy.

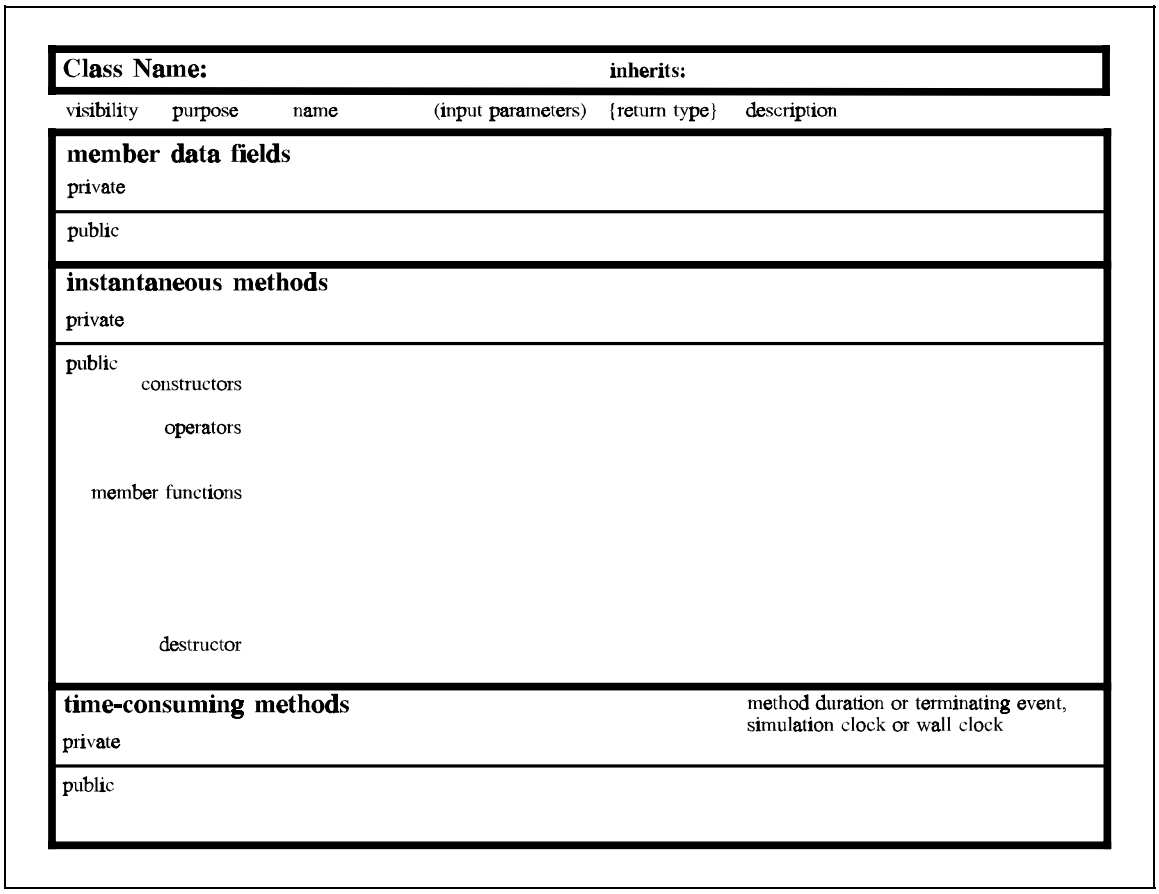

Figure 6.8. OOSPIC class diagram template for ***C++*** class definitions. Separation of class name, data fields, instantaneous methods and time-consuming methods clarifies class functionality and design.

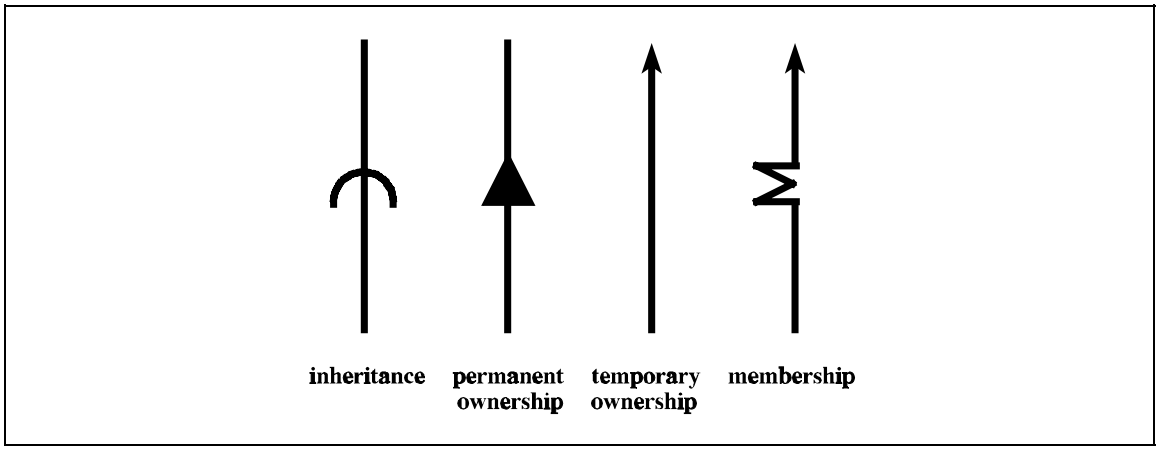

Figure 6.9. Object-Oriented Simulation Pictures (OOSPICs) arrow conventions.

The structure of the general real-time DIS-networked dynamics model presented here appears to be applicable to vehicles of arbitrary type. Documented source code matches the diagrams, equations and algorithms presented in this work (Brutzman 94e). Future work of interest in model design includes determining new parameter values using this model to emulate the characteristics of other underwater vehicles, adapting the model to accommodate dissimilar vehicle entities, porting the model into robot software as an on-board hydrodynamics response predictor, and investigating extensions to the model to support visualization, validation and verification of model relationships against archived or live data records of actual vehicle dynamics performance.

H. SIMULATING ON-BOARD INERTIAL SENSORS

Navigation and position keeping are fundamentally important capabilities for an AUV. Unfortunately the selection, purchase, installation, calibration, testing and interpretation of sensors is time consuming and expensive. A valuable benefit of a networked hydrodynamics model is that it can provide model values for "virtual sensors" which may or may not be physically installed.

There are three types of navigational sensors in common use: sonar, electromechanical and inertial. Navigational sonar sensors either detect the environment or use doppler difference ranging from beacons at known locations, and as such are not appropriately modeled using hydrodynamics parameters. Mechanical or electrical sensors for water flow, depth pressure, plane position, propulsor rpm and battery amp-hour consumption rate are directly represented by model variables for surge $\boldsymbol{u}$, depth $\boldsymbol{z}$ and vehicle state vector values respectively. Normally these sensors are reasonably accurate with zero bias and less than 5-10% error over their operating range. Inertial and gyroscopic detectors can also be modeled but additional considerations pertain.

Inertial navigation sensors are often called "strap-down" systems since they are aligned with vehicle body coordinates and physically fixed to the vehicle frame.

If possible they are kept near the center of gravity to minimize offset moment effects. Complete packages using solid state sensors and integrated circuit processing are now available at relatively low cost, providing angular rate and acceleration values about all three body axes. Many other small inertial units are also available which can provide similar functionality for one or two body axes. Velocity outputs are integrated internally from accelerations, and posture values are then found by integration of velocity.

Accuracy of inertial devices depends on pitch and roll angle estimation and sensitivity to acceleration. Inertial accelerometers are affected both by accelerations on the vehicle and accelerations due to gravity. Since the acceleration due to gravity is about ten times the acceleration of propulsors used by slow speed vehicles, an accurate estimate of vehicle pitch and roll is essential for isolating acceleration components unique to the vehicle. Because both position and rotation estimates are double integrations of accelerations, any noise or error in acceleration estimation is greatly amplified over the passage of time. Proper conversion from local inertial reference frames to geostationary or geocentric inertial reference frames is also necessary (Maloney 88). Additional errors and correction factors all can raise the complexity of the sensor and its model.

Electromechanical and inertial sensors can be precisely modeled by perfect "virtual sensors" using the hydrodynamics model. This is very useful for initial experimentation with navigation functions on the robot. For realistic modeling, however, accurate distributions for sensor bias, error and variance are needed. Such distributions can only be meaningfully applied using specifications and test results for actual hardware. Error models are feasible (Pappas 91) (Brancart 94) and can be modeled statistically (Law, Kelton 91). Simulating "virtual sensors" using the hydrodynamics model is of particular usefulness when evaluating robust vehicle control under variable operating conditions (especially simulated sensor failure). The key to success when producing such simulations will be incorporating statistically valid error models.

I. SPECIAL EFFECTS AND FUTURE WORK: ROBUST CONTROL, TETHER, OCEAN SURFACE, COLLISION DETECTION

The networked real-time availability of this model enables further work in several important research areas. The analysis and design of robust controllers focuses on producing stable performance when controlling multivariable systems with significant uncertainty (Dorato 87). Ordinarily this includes fixed control systems that meet performance measure criteria for specified uncertainty bounds. Example linear control algorithms used in the robot for posture control are included in the robot architecture chapter of this work. More sophisticated controller analysis appears in (Yoerger 85, 90) (Papoulias 89, 91) (Cristi 89) (Healey 89, 92b, 93, 94a) (Fossen 94) and numerous other references. Adaptive control methods and application of machine learning techniques to control are active areas of research (Goheen 87). This work is of particular interest given the paramount importance of vehicle stability despite any potentially chaotic (nonlinear instability) behavior which may emerge due to unforeseen interactions between multiple active controllers. The ability to repeatedly test controllers for yaw, depth, pitch, tracking and hovering while they are operating simultaneously on vehicle hardware in real time in the laboratory is a tremendous research tool provided by this model and the networked virtual world.

Although a tether is not ordinarily used on the NPS AUV, employment of a tether for power supply, task-level mission control or telemetry feedback can be very useful during vehicle testing. Tethers can also be a good way to prepare for using acoustic links, or to reliably test a vehicle in the open ocean prior to autonomous control. It is important to note that the operational characteristics of remotely operated vehicles are often dominated by tether dynamics. Incorporation of a tether injects significant forces and moments into the equations of motion, but tether forces can be realistically modeled (Abel 72) (Brancart 94) (Hover 94). Addition of a general tether model into this underwater vehicle hydrodynamics model is a valuable subject for future work.

Modeling ocean waves and surface interactions are also interesting areas for future work. Model complexity ranges from simple sinusoids to sophisticated numerical models obtained from supercomputer programs analyzing years of empirical oceanographic data (Covington 94) (Fossen 94) (Musker 88) (Blumberg 94). Usually the principle of superposition permits wave and current effects to be injected into the hydrodynamics model solution at the last algorithmic step, implying that highly complex ocean wave and circulation models can be solved off-line or in parallel. Incorporation of high-resolution ocean current models over computer networks is yet another worthy area for future research.

The hydrodynamics model presented here does not include collision effects. Abrupt changes in body acceleration and velocity may require extensions to the temporal integration algorithm. Detecting collisions and points of contact in a highly populated virtual world is a separate active research problem with an extremely high degree of computational complexity. Properly adapting the hydrodynamics algorithm to include realistic collision effects can be done meaningfully if performed in conjunction with the more general virtual world collision detection problem. This is another important area for future research.

J. SUMMARY

The requirements for a general networked underwater vehicle six degree-of-freedom hydrodynamics model are outlined for a robot connected to a virtual world. An overall comparison of vehicle dynamics in other environments shows that the underwater vehicle case is among the most difficult and crucial. No rigorous general model was previously available from a single source which is computationally suitable for real-time simulation of submerged vehicle hydrodynamics. The primary intended contributions of the hydrodynamic model developed here are clarity, correctness, generality, standardized nomenclature and suitability for real-time simulation.

Coordinate systems, variable definitions and coefficient nomenclature are explicitly defined. Kinematics equations of motion reveal constraints between representations in the body coordinate frame and world coordinate frame. Restrictions on Euler angles when pointing vertically are examined. Defining the underwater vehicle dynamics problem as a function of vehicle state vector and hydrodynamics state vector provides precise specifications of algorithm inputs and outputs. Dynamics equations of motion are derived in a form suitable for temporal integration in real time. Dimensionless coefficient values are presented for the NPS AUV and methods are discussed for determining coefficients of other vehicles. After extending previous work, a full set of component dynamics equations of motion are presented, including mass and inertia matrix determination. The dynamics equations of motion are in a form suitable for most existing underwater vehicles. Techniques are demonstrated for modifying these general equations to accommodate different vehicle physical configurations. Since the equations are written to run in real time, it may be computationally feasible to embed them in the robot execution logic as an onboard hydrodynamics response predictor for improved physical control.

Quaternion methods are examined as a possible alternative to Euler angle representations. The use of Distributed Interactive Simulation (DIS) network protocols for communication between virtual worlds imposes special considerations on the hydrodynamic model. An object-oriented networked rigid body dynamics class hierarchy illuminates the design and implementation of the hydrodynamics model. This class hierarchy may also be suitable for other types of networked vehicle models. Simulation of virtual sensors, robust control, tether considerations, ocean surface modeling and collision detection are all examined as possible components of the hydrodynamics model. Numerous considerations in these many areas are pointed out as useful candidates for future research, with the expectation that each can be implemented as compatible networked real-time extensions to the general underwater vehicle dynamics model.